Comments on Inorganic Chemistry
Publication details, including instructions for authors and subscription information:
http://www.informaworld.com/smpp/title~content=t713455155

The Influence of Vibronic Coupling on the Spectroscopic Properties and Stereochemistry of Simple 4- and 6-Coordinate Copper(II) Complexes

Michael A. Hitchman[a]
[a] Chemistry Department, University of Tasmania, Hobart, Tasmania, Australia

To cite this Article Hitchman, Michael A.(1994) 'The Influence of Vibronic Coupling on the Spectroscopic Properties and Stereochemistry of Simple 4- and 6-Coordinate Copper(II) Complexes', Comments on Inorganic Chemistry, 15: 3, 197 — 254
To link to this Article: DOI: 10.1080/02603599408035843
URL: http://dx.doi.org/10.1080/02603599408035843

The Influence of Vibronic Coupling on the Spectroscopic Properties and Stereochemistry of Simple 4- and 6-Coordinate Copper(II) Complexes

MICHAEL A. HITCHMAN
Chemistry Department,
University of Tasmania,
Box 252C, Hobart,
Tasmania 7001, Australia

Received August 3, 1993

Although vibronic Jahn–Teller interactions almost always cause both 4- and 6-coordinate copper(II) complexes to distort significantly away from regular tetrahedral and octahedral geometries, rather different factors influence the size and nature of the distortions. In the former case, the active mode is a bending vibration and this has a very small force constant which is often influenced by factors such as lattice interactions. The size of the distortion therefore varies widely from one compound to another, sometimes causing the limiting planar geometry to be reached. The very low energy of this bending vibration causes several unusual features to occur in the electronic spectrum of the planar $CuCl_4^{2-}$ ion. In particular, the significant temperature dependence of the band maxima and the vibrational fine structure observed at low temperature both imply that in the excited electronic states the complex has an equilibrium geometry distorted towards a tetrahedron. For 6-coordinate copper(II), the overall distortion is always rather large, but the fact that the active Jahn–Teller vibration is doubly degenerate, with discrimination between the components only occurring because of higher order effects, means that the geometry can vary from an elongated tetragonal to a compressed tetragonal octahedron relatively easily, the pathway involving orthorhombic intermediates. In this case, the alteration in geometry is accompanied by a change in the electronic ground state wavefunction. When the six ligands are identical, the elongated geometry is almost always more stable, with the unpaired electron in the $d_{x^2-y^2}$ orbital.

Comments Inorg. Chem.
1994, Vol. 15, Nos. 3 & 4, pp. 197–254
Reprints available directly from the publisher
Photocopying permitted by license only

However, if two *trans* ligands are stronger σ-donors than the other four, either a compressed tetragonal or an orthorhombic geometry may occur, depending upon the size of the ligand field asymmetry, with the unpaired electron in d_{z^2} or, in the latter case, a mixture of the $d_{x^2-y^2}$ and d_{z^2} orbitals. When the metal lies on a crystal lattice site of cubic symmetry, these distortions will occur randomly, producing a time-averaged octahedral geometry. When the site symmetry is lower than cubic, the configurations may differ slightly in energy, and the time-averaged geometry and electronic wavefunction will vary with temperature. The electronic structure is in this case most conveniently studied by electron paramagnetic resonance spectroscopy, and such spectra will be temperature dependent, as will the geometry revealed by X-ray crystal structure determinations. Theoretical models have been developed relating the properties of these complexes to the Jahn–Teller vibronic interactions and ligand field parameters.

Key Words: *copper(II) complexes, vibronic coupling, Jahn–Teller effect, electronic spectra, EPR spectra, variable temperature structures*

I. INTRODUCTION

The Cu^{2+} ion exhibits an unusually rich stereochemistry, with a wide range of coordination polyhedra being represented. However, the regular octahedral and tetrahedral geometries favored for most 6- and 4-coordinate transition metal ions are almost never observed for copper(II). This is because such geometries produce electronically degenerate ground states and, as suggested by the Jahn–Teller theorem,[1] the coupling between vibrational and electronic states renders these shapes unstable with respect to distortions to lower symmetry ligand arrangements. Vibronic coupling of this kind is expected to be particularly strong in Cu^{2+} complexes because for both the octahedral and tetrahedral parent geometries the orbital degeneracy occurs for σ-antibonding orbitals. Simple estimates, based for instance on the angular overlap model (AOM) of the bonding in metal complexes,[2] suggest that the Jahn–Teller coupling coefficients which depend upon σ-bonding interactions should usually be more than four times larger than those involving π-interactions.[3] The Jahn–Teller theorem also implies that several vibrations may act to lower the symmetry of a regular tetrahedral copper(II) complex. However, AOM estimates[4] suggest that one of these should dominate, that which carries the complex towards a planar geometry, and this is indeed confirmed experimentally.[5]

While it is widely accepted that the tetragonally elongated oc-

tahedron, which is probably the most common Cu^{2+} coordination geometry, is caused by Jahn–Teller coupling, it is less commonly appreciated that for 6-coordinate copper(II) complexes other shapes are equally consistent with this theorem.[4] Since the different geometries are connected smoothly by vibrational motion of the ligands, the complexes can change geometry with relatively little input of energy, and tend to be quite "plastic".[6] Moreover, the bending vibration which defines the pathway by which a tetrahedral Cu^{2+} complex distorts is of very low energy, so that 4-coordinate copper(II) complexes are also highly "plastic", and the angles between the metal–ligand bonds vary significantly from one compound to another.

The fact that one of the vibrational modes is of very low energy for many copper(II) complexes means that vibronic coupling may cause the electronic wavefunction to vary significantly over the temperature range 4–300 K. Features such as the *g*-values and the intensity and energy of the bands due to the *d-d* transitions will then be significantly temperature dependent. The "plasticity" of Cu^{2+} complexes also means that their shape in a crystalline compound may be strongly influenced by lattice forces. For instance, the geometry of a charged complex may vary with the counterion. Sometimes the geometry alters sharply in conjunction with a temperature dependent phase transition, and as the electronic wavefunctions are coupled to the nuclear geometry, the optical and electron paramagnetic resonance (EPR, sometimes abbreviated as ESR) spectra will change also. As a result, copper(II) compounds give rise to some spectacular examples of thermochromism.[5,7] Not infrequently the distortions induced by vibronic coupling are statistically disordered in the crystal lattice. Physical measurements which involve the average geometry or electronic wavefunction, such as X-ray diffraction or the EPR spectrum of exchange-narrowed systems, will then yield results indicative of a geometry which differs from that experienced by each Cu^{2+} at the local level, and this has sometimes led to the geometry being identified incorrectly. On occasion, two orientations of a complex in a crystal lattice will differ slightly in energy, and the average geometry will then be temperature dependent.

The purpose of the present article is to discuss the effects of vibronic coupling upon the electronic and geometric structure of

copper(II) complexes, as outlined above. The influence on the optical and EPR spectra is also discussed. These generally provide the most convenient way in which the above features may be investigated experimentally, and before considering particular examples it is appropriate to briefly review the kind of information yielded by each technique.

I.1. Structural Distortions and the Interpretation of Optical and EPR Spectra

Electronic and EPR spectra yield information on the electronic structure of metal complexes from quite different perspectives, and this is well illustrated by the ways in which they may usually be employed to deduce the structures of Jahn–Teller distorted copper(II) complexes. Although the situation is more complicated than this, as discussed in Section II.2, 6-coordinate copper(II) complexes normally distort from a regular octahedral geometry in one of the two ways illustrated in Fig. 1, with two *trans* ligands moving out and four in, or vice versa. The *d*-orbital energies change as shown in Fig. 1, the slight deviations from linearity being due to higher order effects. Three peaks are expected in the electronic spectrum, corresponding to the energy differences E_1, E_2 and E_3. It is apparent that while E_1 provides a good measure of the overall magnitude of the distortion, there is little discrimination as far as the sign of the distortion is concerned. Thus, while d_{z^2}-4s mixing causes E_1 to be somewhat larger for a tetragonal elongation than the corresponding compression, and the relative ordering of the d_{xy} and $d_{xz,yz}$ orbitals interchanges, except when highly resolved spectra allow the peaks to be assigned unambiguously, it is usually difficult to deduce the sign of the Jahn–Teller distortion of a copper(II) complex from its electronic spectrum alone. The direction of the tetragonal axis is sometimes disordered in a crystal lattice, and the direction of the tetragonal bonds may fluctuate dynamically for any particular complex. Because electronic transitions occur on a very short time-scale, it is important to note that the transition energies will be unaffected by these fluctuations, and will reflect the local coordination geometry.

In contrast to optical spectroscopy, which directly involves the excited electronic states, the EPR spectrum probes the nature of

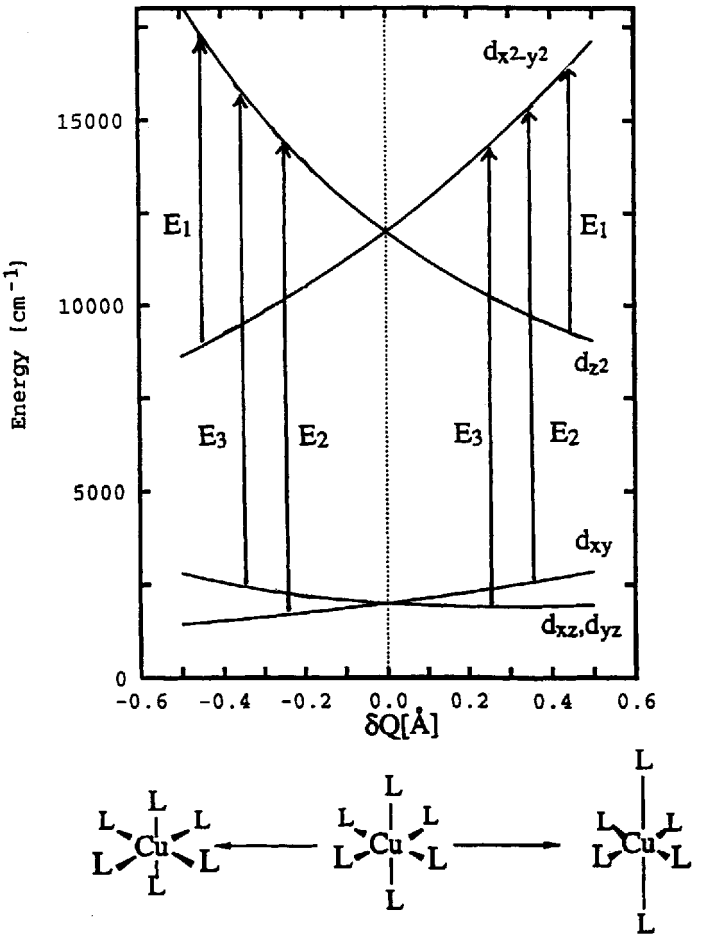

FIGURE 1 Change in energy of the d-orbitals on distorting a 6-coordinate copper(II) complex along the Q_0 coordinate; see Eq. (10) for the relationship between the changes in the normal coordinate and individual bond lengths. The calculations were carried out using the equations given in Ref. 8 for a complex with bonds of length r = 2.1 Å and bonding parameters e_σ = 4000 cm^{-1}, $e_{\pi x}$ = $e_{\pi y}$ = 500 cm^{-1}, e_{ds} = 1000 cm^{-1} in the regular octahedral geometry. It was assumed that the bonding parameters vary as r^{-5}.

the ground state wavefunction, and this changes dramatically on going from an elongated to a compressed tetragonal geometry (Fig. 1). After considering the effects of spin-orbit coupling, first order perturbation theory suggests that the shifts δg from the free electron g-value parallel ($\|$) and perpendicular ($\perp$) to the symmetry axis of the complex are given by

$$\delta g_{\|} = -8\lambda k_{\|}^2/E_2; \quad \delta g_{\perp} = -2\lambda k_{\perp}^2/E_3; \tag{1a}$$

$$\delta g_{\|} = 0.0; \quad \delta g_{\perp} = -6\lambda k_{\perp}^2/E_3 \tag{1b}$$

for an elongated (1a) and compressed (1b) tetragonal geometry. Here, λ is the spin-orbit coupling constant, -828 cm^{-1}, and $k_{\|}$, $k_{\perp}$ are so-called orbital reduction factors which represent the effects of covalency. This means that if the g-tensor of a complex can be measured, the elongated and compressed tetragonal coordination geometries can be distinguished quite unambiguously. The metal hyperfine structure provides similar discrimination, with the addition that the d_{z^2}-4s mixing significantly affects the hyperfine parameters for a compressed tetragonal, but not an elongated tetragonal complex.[9] However, an important limitation of EPR spectroscopy, in contrast to electronic spectroscopy, is the relatively long time-scale of the technique. When the rate of electron exchange between two complexes is more rapid than the energy difference between their EPR resonances, measured in frequency units, then the EPR signals will be "exchange averaged". If the molecular axes are not parallel, the observed g-tensor will then no longer be decided by the local electronic structure of each Cu^{2+} ion. Particular confusion may arise if a complex has a local tetragonally elongated geometry but crystallizes in a 2-dimensional antiferrodistortive arrangement with the long axis of one complex parallel to the short axis of its neighbors. When electron exchange is more rapid than the EPR time-scale, a g-tensor of tetragonal symmetry will be observed:

$$\delta g_{\|} = -2\lambda k_{\|}^2/E_3; \quad \delta g_{\perp} = -5\lambda k_{\perp}^2/E_{2,3} \tag{2}$$

where $\delta g_{\|}$ is parallel to the short Cu-ligand bonds which are aligned with one another, and $\delta g_{\perp}$ is the average of the *local* $\delta g_{\|}$ and $\delta g_{\perp}$-

values. Here, $E_{2,3}$ represents the average of E_2 and E_3. The relative magnitudes of the g-tensor components, $\delta g_{\parallel} < \delta g_{\perp}$, are similar to that expected for a compressed tetragonal geometry (Eq. (1b)), and when the disordered long and short Cu-ligand bond lengths cannot be resolved by X-ray diffraction, this has meant that the EPR spectra of systems of this kind have sometimes been misinterpreted as indicating an ordered arrangement of tetragonally compressed complexes.[10] The non-zero value of $\delta g_{\parallel}$ argues against such an interpretation, but this could be due to vibronic mixing of $d_{x^2-y^2}$ into the d_{z^2} ground state orbital. However, when this occurs the g-values are expected to change markedly with temperature,[11] as discussed in Section III.

To minimize electron exchange, EPR studies often involve the complexes formed when Cu^{2+} is doped into diamagnetic host lattices. Even here, the spectra do not always correspond to the instantaneous structure of the complex. This may exist in two or three forms of identical or similar energy, and exchange between these more rapidly than the EPR time-scale, producing an averaged spectrum. The rate of exchange depends strongly on temperature, so that often an averaged spectrum may be seen at 300 K, but that due to isolated complexes below ~50 K. This type of behavior is characteristic of complexes having identical or similar structures, but differing in their orientation in the crystal lattice. Occasionally, a complex has a vibration of very low energy which mixes an excited state into the ground state by vibronic coupling. Here, the nature of the ground state, and g-values, will vary smoothly with temperature, as the Boltzmann populations of the vibronic energy levels change. Examples of these types of behavior are discussed below, illustrating the fact that it is important to undertake EPR studies of copper(II) complexes over a temperature range whenever there is a possibility of dynamic behavior.

As yet, vibrational spectroscopy has only occasionally been used to study the vibronic energy levels in Jahn–Teller distorted copper(II) complexes.[12] Since this technique offers the potential to measure the relative energies of the vibronic levels directly, it has great potential, and it is to be hoped that recent improvements in instrumentation will lead to a broadening of the data available on these systems.

Although vibronic coupling strongly influences both 4- and

6-coordinate copper(II) complexes, this occurs in rather different ways. It is therefore appropriate to consider examples for each coordination number separately.

II. DISCUSSION

II.1. 4-Coordinate Complexes

A regular tetrahedral geometry yields a $^2T_2$ ground state for a Cu^{2+} complex, and three Jahn–Teller active vibrations may act to lower the symmetry of such a system, two of τ_2 symmetry and one of ϵ symmetry. To first order, the magnitude of the overall displacement Q_0 depends upon the size of the Jahn–Teller coupling coefficient V and inversely upon the force constant k of the vibrational mode (Eq. (3a))[13]:

$$Q_0 = V/k, \tag{3a}$$

$$Q = (\delta_1 - \delta_2 + \delta_3 - \delta_4)/2. \tag{3b}$$

The force constant of the ε mode is much smaller than those of τ_2 symmetry, which means that distortion occurs essentially completely in the former vibration. Moreover, the sense of the distortion always occurs towards a planar ligand arrangement, as pictured in Fig. 2a, the form of the normal coordinate being given in Eq. (3b). The Jahn–Teller coupling coefficients are conveniently estimated in terms of AOM σ and π-antibonding param-

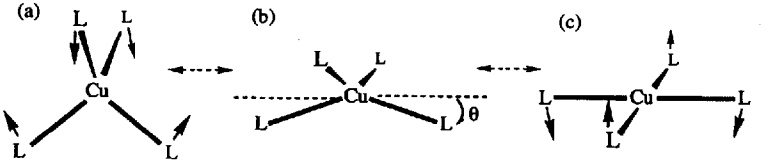

FIGURE 2 (a) The active component of the Jahn–Teller vibration along which distortion occurs for a tetrahedral copper(II) complex. (b) The geometry of D_{2d} symmetry generally observed for 4-coordinate copper(II) complexes. The angular distortion θ of each bond from planarity is indicated. (c) The vibration of β_{2u} symmetry of a planar D_{4h} complex.

eters e_σ and e_π and these have been tabulated by Bacci[4] and Ceulemans *et al.*[14] For the ϵ vibration the coupling coefficient is given by

$$V = 2\sqrt{6}(e_\sigma - e\pi/3)/3r \quad (4)$$

where r is the metal–ligand bond distance. Bonding parameters $e_\sigma = 5030\ \text{cm}^{-1}$, $e_\pi = 900\ \text{cm}^{-1}$ have been reported[15] for a bond distance typical of tetrachlorocuprates, 2.26 Å, yielding the coupling coefficient $V = 3600\ \text{cm}^{-1}\text{Å}^{-1}$. The force constant k of the ϵ vibration has been estimated[16] as ~0.07 mdyneÅ^{-1} and substitution of this into Eq. (3a) suggests a displacement of $Q_0 \approx 1.02$ Å. As each individual ligand moves by $Q/2$ (Eq. (3b)), this corresponds to an opening of each ClCuCl angle from the tetrahedral value to ~134°. This compares favorably with observed values, which typically range from 125° to 133° in compounds where interactions with the counter-cations are not expected to influence the geometry significantly.[17]

Jahn–Teller coupling should thus cause a tetrahedral copper(II) complex to adopt a geometry of D_{2d} symmetry, as depicted in Fig. 2b. However, the very "soft" nature of the active vibration means that distortion along this normal coordinate is very easy, and is readily influenced by lattice forces. In the limit, the complex reaches a planar geometry, as indicated in Fig. 2c. For the $CuCl_4^{2-}$ ion, for which data are available for compounds involving a wide range of counterions, the angle θ (Fig. 2b) varies considerably, and several compounds contain planar $CuCl_4^{2-}$ groups. Here, θ is the angle between each Cu–Cl bond and the xy plane, with x and y lying along the Cu–Cl bonds in the planar limit. The latter all involve bulky amine counter-cations, generally hydrogen bonded to the chloride ligand, and it has been suggested that this hydrogen bonding reduces the electrostatic ligand–ligand repulsion, and hence k, thus allowing the distortion to proceed to the limiting planar geometry.[18] In marked contrast, when Cu^{2+} is doped into ZnO, the Jahn–Teller distortion is effectively quenched,[19] presumably because the force constant of the bending vibration is relatively large in this continuous lattice.

The d-orbital energies vary substantially as a complex distorts from a tetrahedral to a planar geometry, and this is reflected in the electronic transition energies, so that the electronic spectrum

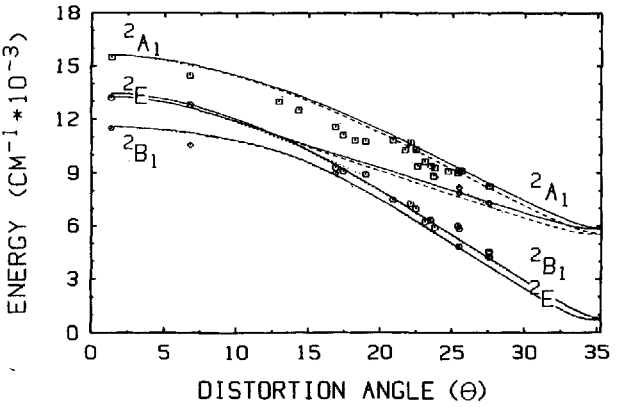

FIGURE 3 The calculated variation of the transition energies of the $CuCl_3^{2-}$ ion as a function of distortion from planarity both neglecting (full lines) and including (dashed lines) a contribution for d-p mixing (e_{dp} = 160 cm^{-1}); see text for the method of calculation and bonding parameters. Here, θ is the angle between each Cu–Cl bond and the *xy* plane, with *x* and *y* lying along the Cu–Cl bonds in the planar limit. Experimental energies of the transitions to the $^2A_1(z^2)$ (squares), $^2E(xz, yz)$ (circles) and $^2B_1(xy)$ (diamonds) are also shown; see Ref. 15 for the sources of the data.

of a 4-coordinate copper(II) complex provides a useful guide to its geometry. The transition energies calculated[15] for the $CuCl_4^{2-}$ ion as a function of the angle θ are shown in Fig. 3, together with the values observed for a range of compounds of known structure. The AOM equations given by Smith[8] were used in the calculation, the parameter values being

$$e_\sigma = 5030\ cm^{-1};\quad e_\pi = 900\ cm^{-1};\quad e_{ds} = 1320\ cm^{-1}.$$

Here, e_{ds} describes the effect of configuration interaction between the d_{z^2} and metal 4s orbitals, this causing a depression of $4e_{ds}$ = 5280 cm^{-1} in the energy of d_{z^2} in the limiting planar complex, decreasing to zero for the tetrahedral geometry. The effect of admixture of the metal *p*-orbitals was also explored by means of an additional parameter e_{dp}, but optimum agreement with experiment occurred when this took a very small value. Spin orbit coupling was included, an effective constant λ = −580 cm^{-1} being used. The plot illustrates not only the wide range of distortions

exhibited by the complex, but also the fact that the AOM provides a self-consistent way of parametrizing the energy levels for the tetrahedral-planar geometric conversion. The rise in the energy of the half-filled $d_{x^2-y^2}$ orbital on going from the tetrahedral to the planar geometry is also expected to cause a progressive increase in the energy of the ligand → metal charge transfer transition, and a significant shift is indeed observed experimentally.[20]

The marked dependence of the electronic transition energies upon ClCuCl bond angle means that the compounds containing planar $CuCl_4^{2-}$ are quite different in color from those in which this complex has a distorted tetrahedral geometry—emerald green, as opposed to yellow. Several compounds undergo a phase transition in which the complex alters from a planar geometry at low temperature to a pseudotetrahedral geometry at high temperature, and the dramatic color change accompanying this makes a spectacular lecture demonstration.[7]

Since the nature of the ground state wavefunction does not alter as a complex distorts from a close to tetrahedral to a planar coordination geometry, no abrupt change in the molecular *g*-values is expected. The *g*-shifts will be described by expressions analogous to those in Eq. (1a), and should progressively decrease as the energy difference between the $d_{x^2-y^2}$ and d_{xy} and $d_{xz,yz}$ orbitals increases (Fig. 3). Certain copper "blue" proteins which contain Cu^{2+} in a highly distorted pseudotetrahedral coordination geometry exhibit temperature dependent *g*-values,[21] and it has been proposed by Bacci[22] that this is caused by a temperature dependent equilibrium between forms having different distortion angles. This hypothesis could be tested by studying the variation of their *d-d* spectra with temperature, as if it is correct the transition energies of the forms should be significantly different.

Unlike the tetrahedral and pseudotetrahedral ligand arrangements, the planar geometry achieved by carrying through the Jahn–Teller distortion to its limit is centrosymmetric. This means that the *d-d* electronic transitions become Laporte forbidden, and the intensity is derived by vibronic coupling involving *ungerade* (*u*)-vibrational modes. The fact that the out-of-plane mode corresponding to the Jahn–Teller active vibration of the parent tetrahedral complex (Fig. 2c) is of very low energy in planar copper(II)

complexes causes a number of unusual features in their optical spectra, and these are outlined below.

II.1.(i) Influence of vibronic coupling on the *d-d* spectra of planar complexes

(a) *Temperature dependence of the d-d-band intensities.* The mechanism by which the electric-dipole intensity of an electronic transition of a centrosymmetric complex is derived by vibronic coupling has been described in detail by various authors.[23,24] An approach which is particularly relevant to the present discussion considers that for each *u*-vibration, the system behaves like a statically distorted complex with the nuclei centred at the root-mean-square (rms) amplitude of the vibration, the selection rules being those for the electric-dipole allowed transitions of a complex of this symmetry. An important consequence of this model is that it implies that the vibronically induced intensity depends only upon the form of the ground state potential surface and is independent of that of the excited state. This result, which has been proved formally by Lohr,[25] is particularly important for planar copper(II) complexes, where it is likely that the equilibrium geometry in the excited electronic states sometimes differs from that in the ground state (see following section). The overall intensity of an electronic transition with the electric vector of polarized light along a particular direction in the molecule is obtained by summing the intensities induced by each active *u*-vibration. In addition, at any particular temperature the intensity induced by each mode is obtained by summing over the vibrational levels with a Boltzmann weighting factor included to take into account the thermal population of each level. The intensity increases as the temperature rises because higher vibrational levels have larger rms amplitudes. For a harmonic potential, this leads to the following expression[23,24] for the intensity I_T at temperature T:

$$I_T = I_0 \coth(h\nu/2kT). \tag{5}$$

Here, I_0 is the intensity at 0 K, h and k are the Planck and Boltzmann constants, and ν is the frequency of the *u*-vibrational mode.

The temperature dependence of a vibronically allowed transition

TABLE I

Vibronic selection rules for a copper(II) complex of D_{4h} symmetry in xy and z polarization.

Excited State	Active Vibration	
	xy	z
$^2B_{2g}(xy)$	ϵ_u	–
$^2E_g(xz, yz)$	α_{2u}, β_{2u}	ϵ_u .
$^2A_{1g}(z^2)$	ϵ_u	β_{2u}

TABLE II

Vibrational energies (cm^{-1}) of the $CuCl_4^{2-}$ ion in $(creatininium)_2CuCl_4$

Mode (D_{4h} Sym.)	Activity	Type	Energy
$\nu_1(\alpha_{1g})$	R	sym. stretch	290
$\nu_2(\beta_{1g})$	R	stretch	[a]
$\nu_3(\alpha_{2u})$	IR	out-of-plane bend	150
$\nu_4(\beta_{2g})$	R	in-plane bend	202
$\nu_5(\beta_{2u})$	–	out-of-plane bend	(75)[b]
$\nu_6(\epsilon_u)$	IR	stretch	308, 290
$\nu_7(\epsilon_u)$	IR	in-plane bend	188

[a]Not observed.
[b]Value estimated by normal coordinate analysis (Ref. 28).

is thus strongly dependent upon the energy of the inducing mode. The fact that bending vibrations are generally lower in energy than stretching vibrations has been used in conjunction with the relative temperature dependence of the bands in different polarizations to make a tentative assignment of the *d-d* spectra of planar copper(II) acetylacetonate complexes.[26] The effects of vibronic coupling on the band intensities of planar $CuCl_4^{2-}$ has been studied in detail in a number of compounds containing this ion.[15,20,27-31] The vibronic selection rules for a copper(II) complex of D_{4h} symmetry are shown in Table I, and the energies of the normal modes obtained[28] from the infrared and Raman spectra of $(creatininium)_2CuCl_4$, a typical compound containing planar $CuCl_4^{2-}$, are given in Table II. The polarized *d-d* spectrum of the (100) crystal face of this compound at various temperatures is shown in Fig. 4, from which it may be seen that the temperature dependence is strongly dependent on the polarization direction. For this compound, when

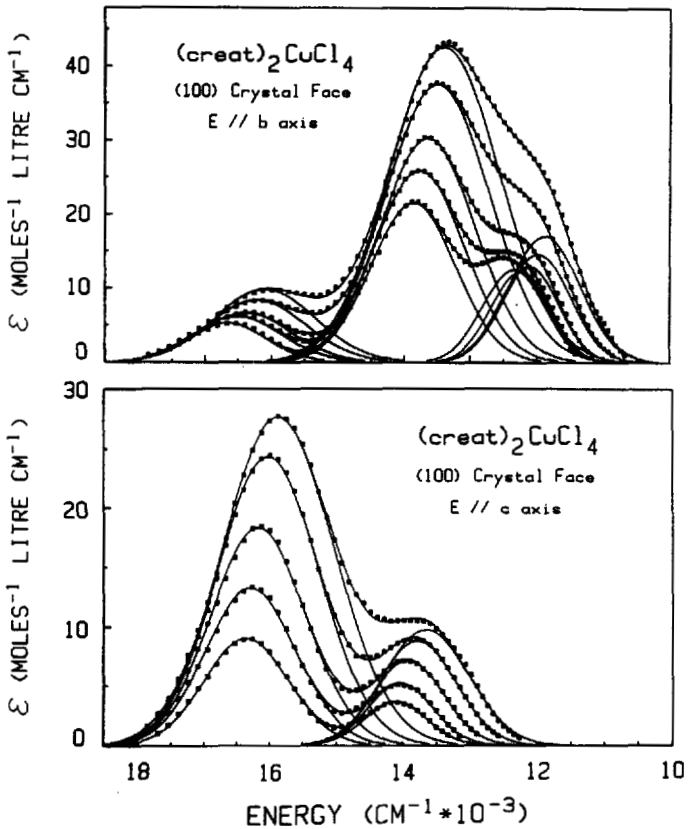

FIGURE 4 Electronic spectra of the (100) crystal face of (creatininium)$_2$CuCl$_4$ with the electric vector of polarized light parallel to the *b* and *c* crystal axes. Experimental points are shown as circles and best-fit Gaussian components, and their sums are shown as lines at temperatures of 10, 50, 90, 140 and 180 K in order of increasing intensity.

the electric vector is parallel to the *c* and *b* axes it is almost exactly parallel and perpendicular to the *z* molecular axis. The band assignments are shown in Table III, as are the average energies of the *u*-vibrational modes inducing intensity into each transition estimated by fitting the temperature dependence of the band intensities obtained by Gaussian analysis to Eq. 5 (Fig. 5). It may be seen from the selection rules that only a single vibrational mode, that of β_{2u} symmetry, is responsible for the intensity of the $^2B_{1g}$

TABLE III

Band assignments and average energies (cm^{-1}) of the vibrational modes inducing intensity into the *d-d* transitions of $(creatininium)_2CuCl_4$.

Excited State	Pol.	Band Max.[a]	Vib. Energy[b]
$^2B_{2g}(xy)$	*xy*	12320	205(20)
$^2E_g(xz, yz)$	*xy*	13880	110(10)
	z	14185	85(20)
$^2A_{1g}(z^2)$	*xy*	16620	155(10)
	z	16360	64(4)

[a]Measured at ~10K.
[b]The uncertainty is given in parentheses.

$\rightarrow {}^2A_{1g}$ transition in *z* polarization, and the observed intensity variation suggests that this has a very low energy, ~64 cm^{-1}. As this transition is both infrared and Raman inactive, the energy cannot be measured directly from the vibrational spectrum, but the estimate of ~75 cm^{-1} obtained by normal coordinate analysis[28] agrees well with that obtained from the optical spectrum. The low energy is consistent with the fact that this vibration carries the complex towards a tetrahedral geometry (Fig. 2c), the preferred stereochemistry in the absence of Jahn–Teller coupling.

Modes of ϵ_u symmetry are vibronically active for the transitions $^2B_{1g} \rightarrow {}^2B_{2g}$ and $^2B_{1g} \rightarrow {}^2A_{1g}$ in *xy*, and $^2B_{1g} \rightarrow {}^2E_g$ in *z* polarization, and planar $CuCl_4^{2-}$ has two vibrations of this symmetry. The energies derived from the temperature dependence of the band intensities for the first two transitions, 205 cm^{-1} and 155 cm^{-1}, respectively, are not too dissimilar from that of the lower energy, out-of-plane mode of ϵ_u symmetry, 188 cm^{-1}, suggesting that most of the intensity is derived by coupling with this vibration. However, the $^2B_{1g} \rightarrow {}^2E_g$ transition in *z* polarization exhibits a temperature dependence consistent with an active vibration of considerably lower energy than either metal–ligand ϵ_u vibration, ~85 cm^{-1}. Possibly, coupling with low energy lattice vibrations may add to the intensity in this case. In *xy* polarization, this transition gains intensity by coupling with modes of β_{2u} and α_{2u} symmetry, and in agreement with this the "average" vibrational energy derived from the temperature dependence of the intensity, 110 cm^{-1}, lies between the energy of the β_{2u} mode, ~64 cm^{-1}, and that of the α_{2u} vibration, 150 cm^{-1}. The observed intensity variation can be sim-

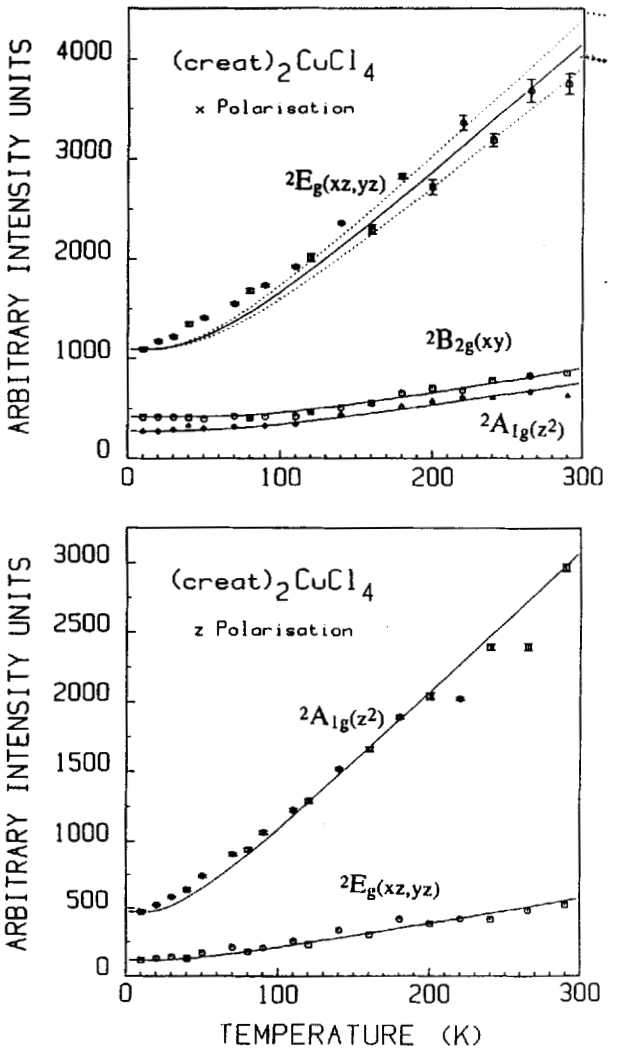

FIGURE 5 Temperature dependence of the intensities obtained by Gaussian analysis of d-d bands of (creatininium)$_2$CuCl$_4$. The full lines show the temperature dependence calculated (Eq. (5)) using the vibrational energies shown in Table III. For the transition to the $^2E_g(xz, yz)$ state in x polarization the intensity is the sum of that induced by the modes of α_{2u} and β_{2u} symmetry, with 75 ± 6% of the intensity at 0 K being derived from the former mode, and the dashed line indicates the range of calculated intensities implied by this uncertainty.

ulated satisfactorily assuming that 75% of the intensity at 0 K is derived from the α_{2u} vibration, the remainder coming from the β_{2u} mode (Fig. 5).

Generally similar results have been obtained from analysis of the temperature dependence of the *d-d* band intensities of the planar $CuCl_4^{2-}$ ion in other compounds,[27] and all-in-all it appears that for this system at least, the simple vibronic coupling model explains this aspect of the spectra reasonably well. However, other features still await interpretation. In particular, although the way in which the intensities increase as the temperature is raised may generally be explained satisfactorily, little attempt has yet been made to interpret the intensity-inducing activity of the different modes, i.e., the relative values of I_0 produced by the different *u*-vibrations. It has been pointed out by Solomon[20] that the fact that the spectra are considerably more intense in *xy* than in *z* polarization may be explained by the relative energies of the charge transfer transitions from which intensity is "borrowed". However, it is not clear why, for instance, the in-plane mode of ϵ_u symmetry is apparently vibronically inactive in producing intensity in the spectrum of $CuCl_4^{2-}$.

As discussed above for the mode of β_{2u} symmetry, analysis of the temperature dependence of band intensities can sometimes provide useful information on the energies of vibrations which cannot be obtained directly from infrared or Raman spectroscopy. In certain favorable cases, such as planar $CuCl_4^{2-}$, the anharmonicity of the inducing vibration may even be investigated. The variation of the intensity as a function of temperature for the $^2B_{1g} \rightarrow {}^2A_{1g}$ transition of the planar $CuCl_4^{2-}$ ion in $(methadonium)_2CuCl_4$, $(metH)_2CuCl_4$ in *z* polarization is shown in Fig. 6, together with the "best-fit" dependence (Eq. (3)) obtained[29] with a β_{2u} energy of 65 cm^{-1}. While the fit is generally reasonable (dashed line), the intensity starts to increase at a lower temperature than is predicted by the simple expression, but rises less steeply than is predicted at higher temperatures. This behavior can be explained[29] if the β_{2u} mode is slightly anharmonic, and a potential of the form

$$V(\xi) = 0.5\xi^2 + \exp(-0.5\xi^2); \quad h\nu = 60 \text{ cm}^{-1} \qquad (6)$$

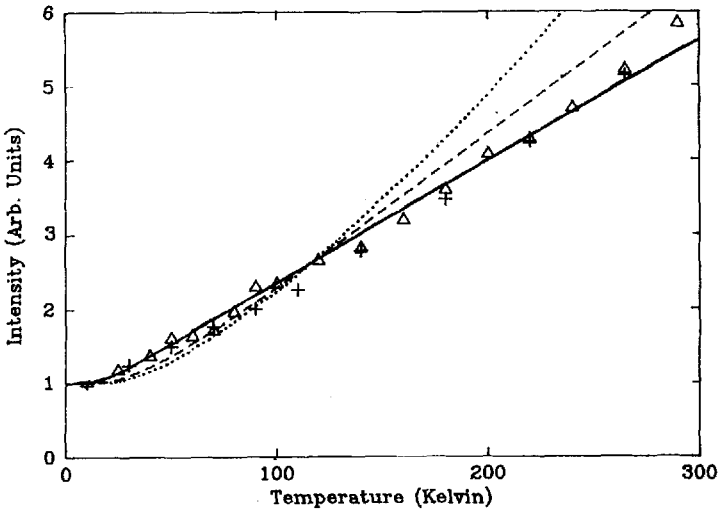

FIGURE 6 Calculated and observed temperature dependence of the transition to the $^2A_g(z^2)$ state of $(metH)_2CuCl_4$ in z polarization; triangles and crosses refer to data from different crystals. The full and dashed lines show the temperature dependence calculated using anharmonic and harmonic potentials for the β_{2u} mode (see text for details). The dotted line shows the temperature dependence assuming the transition moment integral is expanded to 2nd order (see Ref. 29 for details).

improves the fit considerably (Fig. 6, full line). Here, ξ is a dimensionless coordinate related to the normal coordinate (see Ref. 29 for details). The form of this potential surface is shown in Fig. 7B, from which it may be seen that the anharmonicity is quite modest. An alternative explanation for deviations of the intensity variation of vibronically allowed transitions from the behavior predicted by the simple "coth rule" has been put forward by Ferguson,[32] namely, that the electronic transition moment should be expanded to second order. However, this suggests that the intensity should rise more rapidly with temperature than is predicted by Eq. 3, which is the opposite of what is observed experimentally in this case (Fig. 6, dotted line).

(b) *Temperature dependence of the band maxima.* A particularly striking feature of the temperature dependence of the *d-d* spectra of planar $CuCl_4^{2-}$ is the large red-shifts of the band maxima which

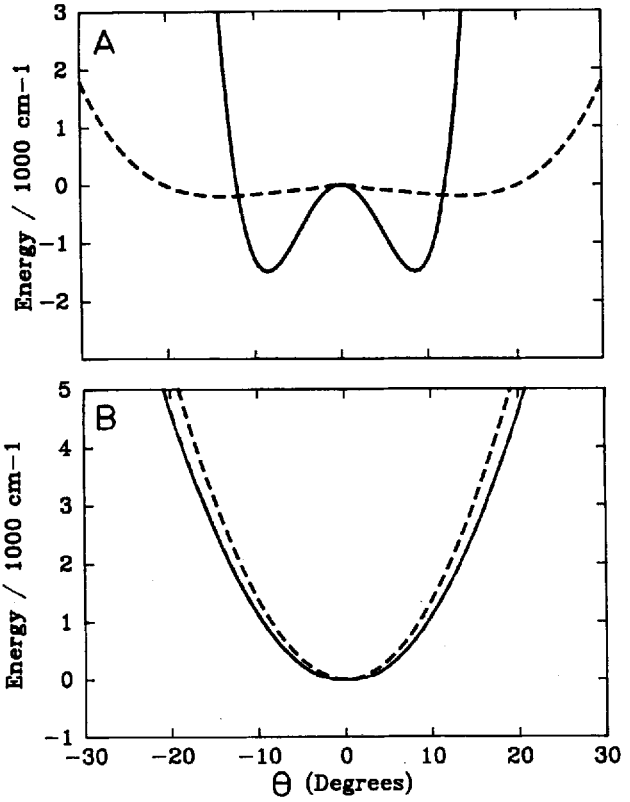

FIGURE 7 Potential surfaces of the $CuCl_4^{2-}$ ion in $(metH)_2CuCl_4$ along the β_{2u} coordinate in (A) the $^2A_{1g}(z^2)$ excited state and (B) the ground state. In (A) the dashed curve is that calculated using the AOM and the full curve is that giving agreement with the experimentally observed temperature dependence of the energy of the band maximum. In (B) the dashed line is the harmonic potential corresponding to a vibrational energy of 65 cm^{-1} and the full line corresponds to the anharmonic potential given by Eq. (6).

occur as the temperature rises from 15 K to 300 K (Fig. 4). The simple model of vibronic coupling does predict a red-shift, by virtue of the selection rule which requires that the vibrational quantum number v of the inducing mode must change by 1 between the ground and excited electronic states.[23,24] At low temperature the complex will be in the $v = 0$ state, and each band will consist of

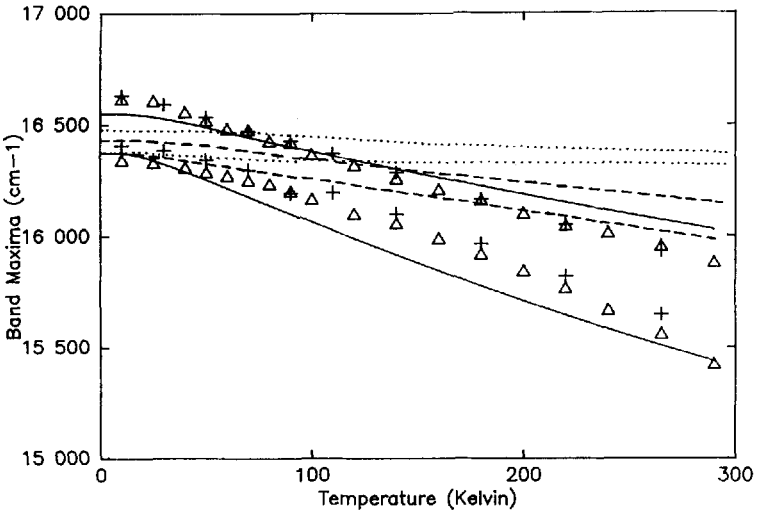

FIGURE 8 Temperature dependence of the band maximum of the transition to the $^2A_{1g}(z^2)$ excited state of $(metH)_2CuCl_4$. The higher energy experimental points and calculated curves refer to xy polarization and the lower energy ones to z polarization. The dotted lines show the behavior calculated assuming identical harmonic potential surfaces in the ground and excited states (except for a displacement in the α_{1g} mode). The dashed lines show the shifts calculated using an anharmonic ground state potential surface and the excited state surfaces estimated using the AOM, while the full lines show those estimated using a more highly distorted excited state potential surface (Figs. 7B and 7A).

a progression in the totally symmetric α_{1g} mode built upon an electronic origin E_0 plus 1 quantum of the inducing vibration. At high temperatures thermal population of $v = 1, 2$ etc. levels of the ground state will occur, giving rise to "hot bands" built upon origins at $E_0 - 1$ and $E_0 + 1$ quantum of the inducing vibration. However, this mechanism can only induce red-shifts comparable to the energies of the inducing vibration, ~60–300 cm^{-1}, which is considerably smaller than those observed for planar $CuCl_4^{2-}$, as may be seen from the temperature dependence of the band maxima of the $^2B_{1g} \rightarrow {}^2A_{1g}$ transition of $(metH)_2CuCl_4$ shown in Fig. 8. It might be thought that the shifts are caused by a contraction of the Cu–Cl bonds upon cooling. While such mechanism might be feasible for a lattice involving bridging ligands, for an isolated complex it implies an anharmonicity in the totally symmetric α_{1g} stretching

vibration. This is of too high an energy (~270 cm^{-1}) for thermal population to influence the band shape significantly at temperatures below 300 K; moreover, the vibrational fine structure observed at low temperature shows the α_{1g} vibration to be quite harmonic in the excited electronic states.[28]

A more likely cause of the shifts is that the equilibrium nuclear geometry in the excited electronic state differs significantly from that in the ground state. To first order, such a change may only occur for totally symmetric vibrations (and Jahn–Teller active vibrations, in the case of orbitally degenerate electronic states), and it is neglected in simple treatments of the effects of vibronic coupling upon electronic spectra.[23,24] However, the very low energy of the β_{2u} vibration of planar $CuCl_4^{2-}$ means that a distortion in this mode seems feasible, particularly as this vibration carries the complex into the pseudo-tetrahedral geometry which is the most stable ligand arrangement of this complex in the absence of lattice forces. Simple calculations of the variation in energy of $CuCl_4^{2-}$ in each excited electronic state as a function of distortions along the normal coordinates of the planar complex have been carried out using the AOM, and these suggest[29] that whereas the potential surfaces of the other normal coordinates simply correspond to a lowering of the force-constants in each excited electronic state, for the β_{2u} vibration shallow minima corresponding to a highly distorted tetrahedral ligand arrangement occur (Fig. 7A). While such a distortion does produce a larger red-shift than the simple model of vibronic intensity "stealing" (Fig. 8), it is considerably smaller than that observed experimentally, as may be seen from the calculated (dashed line) and observed shifts shown in Fig. 8. The observed changes in band shape are reproduced satisfactorily (Figs. 8 and 9) by an excited state potential surface more sharply localized at a distorted tetrahedral geometry (Fig. 7A). This provides an excellent fit to the change in bandshape in *z* polarization, where the intensity is derived from the mode in which the distortion occurs. The bandshape change in *xy* polarization is less well reproduced, which is not surprizing, as here the intensity is derived from vibrations other than the β_{2u} mode (see preceding section). It should be noted that the distorted upper potential surface reproduces not only the temperature dependence of the band maxima, but also the sign and magnitude of the energy separation between these in the different polarizations. It is not unreasonable that the ligand-field calculations

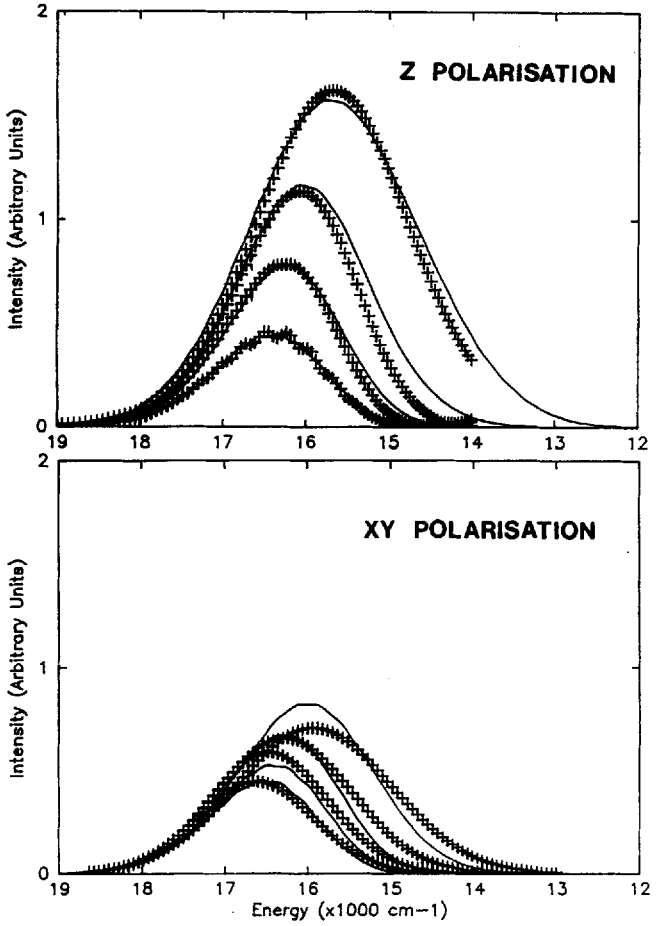

FIGURE 9 Observed (crosses) and calculated (full lines) bandshapes of the transition to the $^2A_{1g}(z^2)$ excited state of $(metH)_2CuCl_4$. at temperatures of, in order of increasing intensity, 10, 70, 140 and 265 K. The contribution to the intensity from lower energy bands has been subtracted. The calculations were carried out using the ground and excited state potential surfaces shown by the full lines in Fig. 7 (see Ref. 29 for details).

give a rather poor representation of the form of the upper potential surface, since it is likely that this is strongly influenced by coupling with ligand → metal charge-transfer states, which lie only ~8000 cm^{-1} higher in energy than the excited *d*-state.[20]

(c) *Vibrational fine structure*. The *d-d* spectra of several compounds containing planar $CuCl_4^{2-}$ are unusual in showing vibrational fine structure at low temperature,[27,28,30,31] and this greatly helps elucidate the nature of the vibronic coupling involved in the electronic transitions.

At low temperature, the bands due to the $^2B_{1g} \rightarrow {}^2B_{2g}$ and $^2B_{1g} \rightarrow {}^2A_{1g}$ transitions of $(metH)_2CuCl_4$ both consist of a single progression of energy ~265 cm^{-1}, this clearly being in the totally symmetric α_{1g} mode which has an energy of 275 cm^{-1} in the ground state.[28] Such a progression is exactly what is predicted by group theory, which suggests non-degenerate excited electronic states may undergo displacements only in normal coordinates of α_{1g} symmetry. However, as discussed in the preceding section, the temperature dependence of the band shapes suggests that for this compound a displacement also occurs in the β_{2u} mode in each excited state, to give an equilibrium nuclear geometry of D_{2d} symmetry, and the question arises as to whether the observed vibrational fine structure is consistent with this hypothesis.

As all of the intensity of the $^2B_{1g} \rightarrow {}^2A_{1g}$ transition in *z* polarization is derived by coupling with the β_{2u} vibration, it is possible to estimate the electronic spectrum associated with the individual vibrational levels of the ground state by analyzing the way in which the bandshape changes with temperature, and this has been undertaken[30] over the temperature range 13–100 K. The spectra due to the transitions originating from the lowest $v = 0$ and second lowest $v = 1$ vibrational levels of the β_{2u} mode are shown in Fig. 10A, after subtracting out the absorption due to the other electronic transitions. It was found that the distorted excited state potential surface giving optimum agreement with the shift in band maximum with temperature (see preceding section) also produced band shapes for the $v = 0$ and $v = 1$ spectra in good agreement with experiment. Here, the slight anharmonicity in the β_{2u} mode in the ground state was ignored, and a vibrational energy of 53 cm^{-1} was used, this corresponding to the harmonic potential producing optimum agreement with the change in intensity between 13 K and 100 K. The intensity of the band originating from the $v = 1$ level derived from the above analysis was found to be 2.9 times larger than that originating from the $v = 0$ level, in good agreement with the factor

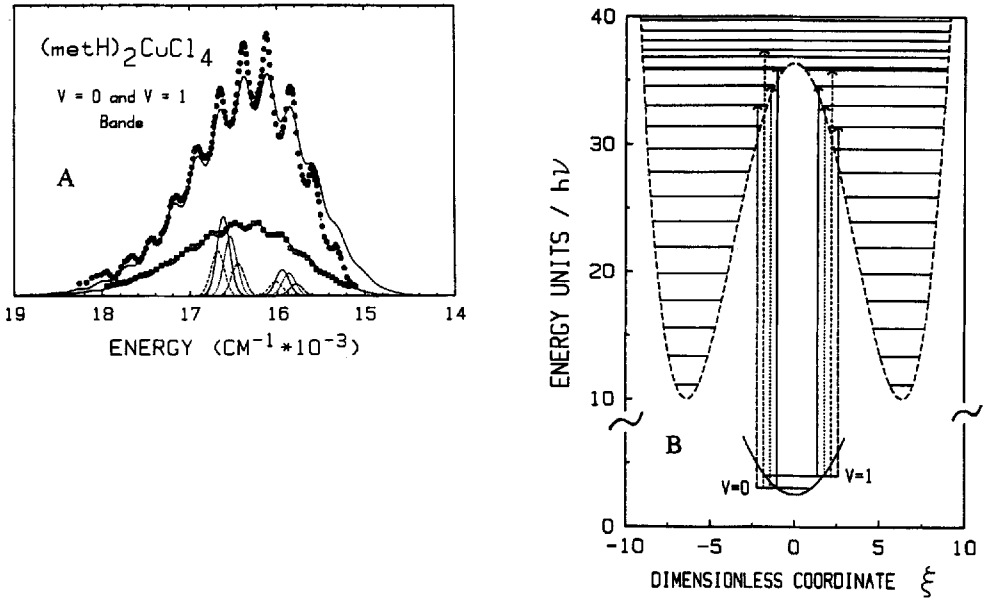

FIGURE 10 (A) Observed (circles) and calculated (full lines) bandshapes of the $^2A_{1g}(z^2)$ transition of $(metH)_2CuCl_4$. in z polarization originating from the $v = 0$ (lower curve) and $v = 1$ (upper curve) levels of the β_{2u} mode at 10 K. The contribution to the intensity from lower energy bands has been subtracted. The four most intense vibronic origins are depicted using different line types for arbitrary single components of the α_{1g} progression. A basic half-width/half-height of 56 cm^{-1} was used in the simulations. (B) Ground and $^2A_{1g}(z^2)$ excited state potential surfaces in the β_{2u} mode indicating the transitions responsible for the most intense components contributing to each peak in (A).

of 3 predicted by the vibronic intensity model (note that while the distortion of the geometry of the excited state affects the band shape, it is not expected to influence the band intensity).[25] The reproducibility of the results was checked by estimating the band-shapes using spectra measured at different sets of temperatures.

The simple model of vibronic coupling, in which the ground and excited states have identical geometries except for a displacement in the α_{1g} mode would suggest that the nth component of the $v = 0$ band consists of a single peak, corresponding to the excitation to the $v = 1$ level of the upper state plus n quanta of the α_{1g} mode in the excited state. Early interpretations of the fine structure observed for $(metH)_2CuCl_4$ and similar compounds followed this approach,[27,28] and the relative intensities of the members of the progression, corresponding to excitations to the $v = 0, 1, 2$, etc. levels of the excited electronic state were used to derive the displacement in the α_{1g} mode accompanying the electronic excitation. When the excited state is also displaced in the β_{2u} coordinate, as proposed above, then a progression is also expected in this mode. This suggests that for $(metH)_2CuCl_4$, each member of the progression actually consists of a band in the β_{2u} vibration, though the energy separation between these is too small to allow them to be resolved (Fig. 10A). The transitions giving rise to the four most intense components are illustrated for the $v = 0$ and $v = 1$ bands in Fig. 10B. It may be seen that the greater amplitude of the $v = 1$ ground state level means that the maximum vibronic overlap tends to occur with lower energy vibrational levels of the upper state, and it is this trend which is the basic cause of the large red-shift which accompanies the thermal occupation of the higher vibrational levels of the ground electronic state (see preceding section).

This model thus ascribes the overall band structure observed at low temperature for $(metH)_2CuCl_4$ to a progression in the totally symmetric α_{1g} mode, but built upon a band in the β_{2u} mode, rather than a single vibronic origin, as would be the case in the simple model of vibronic coupling. The relative intensities of the members of the α_{1g} progression are related to the displacement δQ (α_{1g}) between the ground and excited states in this mode. The simulations shown in Figs. 8 and 10 were carried out using δQ $(\alpha_{1g}) \approx 0.212$ Å, corresponding to an expansion of each Cu–Cl bond of

$\delta r \approx 0.106$ Å in the antibonding upper state. A general expression describing the change in bond lengths accompanying the rearrangement of the *d*-electrons in a transition metal complex has been reported.[33] This relates the relative energy of the states ΔE to the force constant k of the normal coordinate in which the displacement occurs. Assuming that the energy difference depends inversely upon some power n of the metal–ligand bond length r, then for the totally symmetric mode the bond length difference δr is given by

$$\delta r \approx nm\Delta E/(krN). \tag{7}$$

Here, m is the number of electrons involved in the rearrangement, and N is the number of ligands. The ligand-field splitting in a complex has been shown[34] to vary inversely as approximately the fifth power of the bond length, i.e., $n \approx 5$, and for the electronic transitions of $CuCl_4^{2-}$ $m = 1$ and $N = 4$. Substituting the energy of the $^2B_{1g} \rightarrow {}^2A_{1g}$ transition, 16560 cm^{-1}, together with the force constant of the α_{1g} mode, 1.59 mdyneÅ^{-1}, and the Cu–Cl bond length, 2.27 Å, into Eq. (7) yields $\delta r = 0.114$ Å, in excellent agreement with the value of $\delta r \approx 0.106$ Å from the bandshape analysis. Application of a similar procedure to the $^2B_{1g} \rightarrow {}^2B_{2g}$ transition implies an increase of 0.079 Å in each Cu–Cl bond in the excited state. Substitution of the observed value $\Delta E = 12150$ cm^{-1} into Eq. (7) yields the estimate $\delta r = 0.085$ Å. Agreement is again excellent, and it may be noted that this approach ascribes the smaller bond length difference associated with the latter excited state to the fact that it is more weakly antibonding than the $^2A_{1g}$ state.

The fact that the above interpretation suggests that each component of the $^2B_{1g} \rightarrow {}^2A_{1g}$ and $^2B_{1g} \rightarrow {}^2B_{2g}$ bands in the spectrum of $(metH)_2CuCl_4$ itself consists of an unresolved set of peaks to different levels of the β_{2u} mode in the excited state raises the possibility that these might perhaps be resolved in other compounds. The band due to the $^2B_{1g} \rightarrow {}^2A_{1g}$ transition in the low temperature electronic spectrum of (methylphenethylammonium)$_2CuCl_4$ consists of several progressions in the α_{1g} mode, and it was originally suggested that these were due to coupling with a combination of metal–ligand and lattice vibrations.[27] An alter-

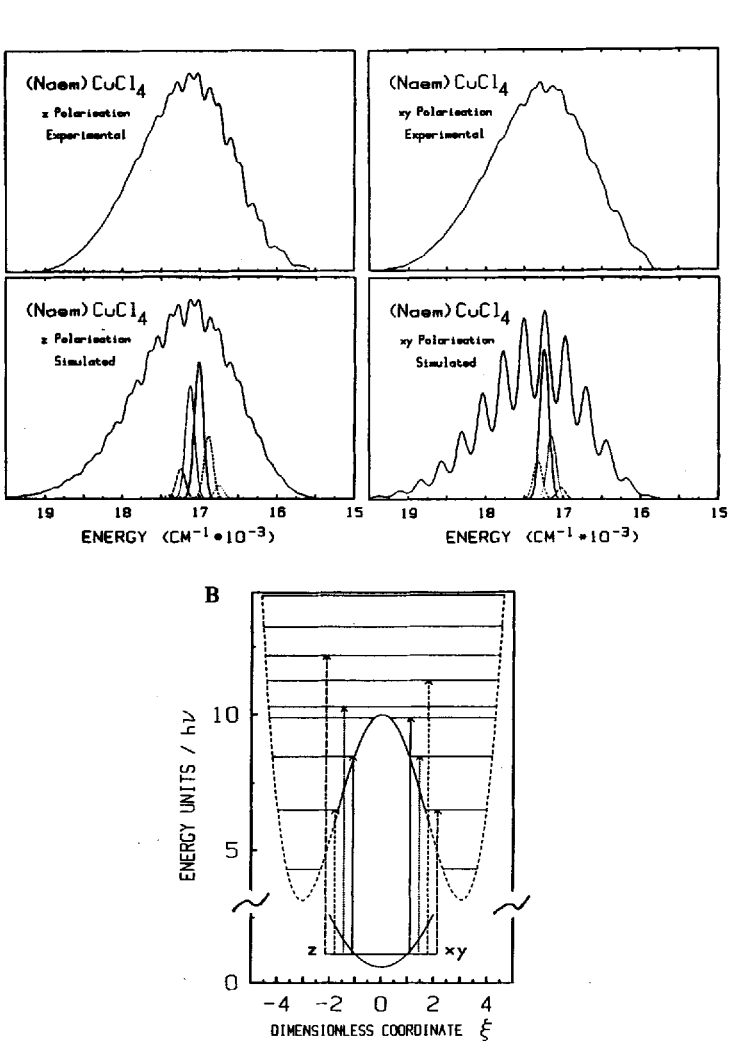

FIGURE 11 (A) Experimental and simulated bandshapes for the $^2A_{1g}(z^2)$ transition of (Naem)$CuCl_4$ at 10 K. The contribution to the intensity from lower energy bands has been subtracted. The four most intense vibronic origins are depicted using different line types for single components of the α_{1g} progressions. A basic half-width/half-height of 58 cm^{-1} was used in the simulations. (B) Ground and $^2A_{1g}(z^2)$ excited state potential surfaces in the β_{2u} mode indicating the transitions responsible for the vibronic origins shown in (A) above.

native explanation is that the complex pattern is in fact due to the resolution of the transitions to individual levels of the metal–ligand β_{2u} vibration in the excited electronic state. Unfortunately, the orientation of the planar $CuCl_4^{2-}$ groups in the crystal lattice of this compound did not allow the molecular spectrum to be resolved accurately, preventing a detailed analysis of the fine structure. However, a complex pattern is also observed on the band due to the $^2B_{1g} \rightarrow {}^2A_{1g}$ transition in the spectrum of the planar $CuCl_4^{2-}$group in *N*-(2-Ammonioethyl)morpholiniumCuCl$_4$, (Naem)CuCl$_4$ (Fig. 11A).[31] The structure observed in *z* polarization is particularly important, as here the simple model of vibronic coupling, in which the ground and excited states have identical shapes, implies that the band should consist of just one progression, as only one vibration, the β_{2u} mode, is active in inducing intensity. The bandshape can be simulated satisfactorily assuming a distortion in the β_{2u} mode in the excited state corresponding to $\theta_{min} \approx 4.8°$ (Fig. 11B).[31] This potential surface also implies a temperature dependence of the band maximum in good agreement with experiment. The reason that the individual transitions to the upper β_{2u} levels are resolved in (Naem)CuCl$_4$, but not in (metH)$_2$CuCl$_4$, appears to be the smaller distortion in the excited state of the former compound. This means that the more intense components of the β_{2u} band are due to transitions to levels close to the saddlepoint between the two minima of the upper state, and these have rather uneven energy spacings (Fig. 11B). For the larger distortion in the upper state of (metH)$_2$CuCl$_4$, $\theta_{min} \approx 8°$, the more intense transitions occur to the approximately equally spaced vibrational energy levels of the downward sloping portion of the upper state (Fig. 7), and these give rise to a regular, approximately Gaussian shape for the β_{2u} band (Fig. 10).

The vibrational structure in the $^2B_{1g} \rightarrow {}^2A_{1g}$ band of (Naem)CuCl$_4$ in *xy* polarization is simulated rather poorly using the excited state potential surface giving optimum agreement with the *z* spectrum (Fig. 11A), though reasonable agreement was obtained with other similar potential surfaces.[31] Poor agreement was also obtained with the observed temperature dependence of the band maximum in *xy* polarization. Note that agreement is expected to be poorer in this polarization as the intensity is derived by coupling with modes of ϵ_u symmetry, rather than with the β_u vibration. Moreover, when

the distortion in the excited state is small, the nature of the vibrational fine structure and temperature dependence of the band maximum was found to be quite sensitive to the form of the excited state potential surface. This is in marked contrast to the situation when the distortion is relatively large, as appears to be the case for $(metH)_2CuCl_4$, when these features are rather insensitive to the form of the upper potential surface. The failure to reproduce the form of the vibrational fine structure and the temperature dependence of the band maxima of $(Naem)CuCl_4$ in both polarizations using a unique potential surface for the upper electronic state is not unexpected when it is remembered that this is represented in a very simple manner in the calculations. The potential surface represents the variation of the energy of the complex as a function of a displacement along the β_{2u} normal coordinate, and it is very probable that this will be influenced by the environment of the $CuCl_4^{2-}$ group in the crystal lattice (it is just this sort of effect acting on the *ground state* potential surface which causes the wide range of distortions observed for this complex when it is co-crystallized with different counter-ions; see Section II.1). The upper potential surfaces could therefore be considerably less simple than those pictured in Figs. 7 and 11B. The influence which the lattice is expected to have upon the excited state potential surfaces of the planar $CuCl_4^{2-}$ ion provides a plausible explanation of the fact that while the energies and relative intensities of the *d-d* bands are very similar for the four compounds so far reported to contain this group, the nature of the vibrational fine structure observed at low temperature varies dramatically. All in all, while it seems likely that in each planar complex the equilibrium nuclear geometry in the excited electronic states is distorted from D_{4h} to an essentially D_{2d} symmetry, with this distortion being greater for $(metH)_2CuCl_4$ than for $(Naem)CuCl_4$, it must be stressed that at this stage the precise form of each upper potential surface can only be determined quite approximately.

Vibrational fine structure is generally not observed in the electronic spectra of mixed ligand copper(II) complexes, presumably because two or more modes of α_{1g} symmetry then occur, and progressions in these overlap to produce a featureless band envelope. Exceptions are several planar, 4-coordinate complexes of the form *trans* CuL_2Cl_2, where L represents an oxygen donor ligand

such as H_2O[35] or an aromatic amine.[36] Here, complex patterns are observed, due to interference between two α_g progressions, one predominately involving motion of the chloride ligands, and the other in that involving motion of the ligand L.

II.2. 6-Coordinate Complexes

The Jahn–Teller theorem predicts that a regular octahedral geometry is unstable for a copper(II) complex. Only one vibration is Jahn–Teller active, but this is doubly degenerate, the form of the two components being illustrated in Fig. 12B.[6,13] The result of

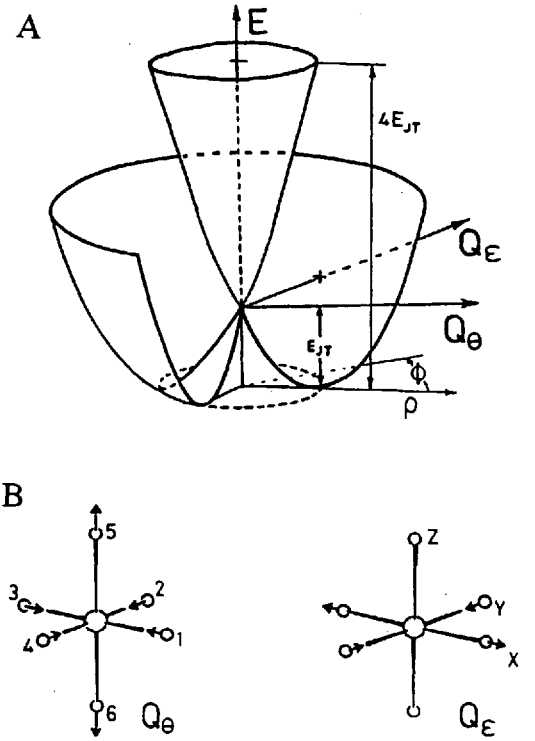

FIGURE 12 (A) "Mexican hat" potential surface which results from the Jahn–Teller coupling between an E_g electronic state and ϵ_g vibrational mode. (B) Forms of the two components of the Jahn–Teller active ϵ_g vibration.

the coupling between the ^2E_g electronic and ϵ_g vibrational states is conventionally represented by the "Mexican hat" potential surface illustrated in Fig. 12A. At this level of approximation, the overall displacement $\rho = V/k$ and the Jahn–Teller stabilization energy $E_{JT} = V^2/2k$, with the splitting of the ^2E_g level being $4E_{JT}$; here V is the linear coupling coefficient and k the force constant of the ϵ_g vibration. The coefficient V depends upon the σ-antibonding energy of the e_g d-orbitals, Δ', and if this varies inversely as the 5th power of the metal–ligand bond distance r, the following relationship results to first order[37]:

$$V \approx 5\Delta'/\sqrt{12}r. \tag{8}$$

For a typical ligand such as H_2O, $\Delta' \approx 11500\ cm^{-1}$, and assuming $r = 2.1$ Å and an energy of 230 cm^{-1} for the ϵ_g mode yields the estimate $V \approx 7900\ cm^{-1}Å^{-1}$. This suggests an overall displacement $\rho \approx 0.276$ Å, and a splitting of the ^2E_g state of $4E_{JT} \approx 4400\ cm^{-1}$. With these approximations, although ρ and the ^2E_g splitting are of the right order of magnitude, both are underestimated by ~50%[37]; a higher value for the energy of the ϵ_g mode, as has been assumed in later studies of the $Cu(H_2O)_6^{2+}$ ion,[38] would increase this discrepancy.

To 1st order, distortions along both components of the ϵ_g vibration are equally favorable, so that not only are elongated and compressed tetragonal geometries energetically equivalent, but an orthorhombic geometry is equally possible. The position of the complex in the Mexican hat surface can be represented by the angle φ (Fig. 12A), the relative displacements along the components being given by[13]

$$Q_\theta = \rho \cos \phi; \quad Q_\epsilon = \rho \sin \phi. \tag{9}$$

Here, the displacements of the six individual ligands δ_{x1}, etc. are given by (Fig. 12)

$$\begin{aligned} Q_\theta &= (2\delta_{z5} + 2\delta_{z6} - \delta_{x1} - \delta_{y2} - \delta_{x3} - \delta_{y4})/\sqrt{12}; \\ Q_\epsilon &= (\delta_{x1} - \delta_{y2} + \delta_{x3} - \delta_{y4})/2, \end{aligned} \tag{10}$$

and the corresponding electronic part of the ground state wavefunction ψ by

$$\psi = d_{x^2-y^2} \cos(\phi/2) + d_{z^2} \sin(\phi/2). \quad (11)$$

At $\phi = 0$, the complex is distorted purely along Q_θ, with a geometry of tetragonal symmetry elongated along z and the unpaired electron in $d_{x^2-y^2}$. As ϕ increases, the ligands along z and x approach the Cu^{2+}, while those along y move away, until at $\phi = 30°$ the ligand displacent is purely in Q_ϵ with the Cu–L bond lengths along y midway between those along x and z, and the electronic part of the ground state a mixture of $d_{x^2-y^2}$ and d_{z^2}. When $\phi = 60°$ the ligand displacent is again purely in Q_θ, but with the bonds along x now forming the symmetry axis of a compressed tetragonal structure and the unpaired electron in d_{x^2}. As ϕ increases further, the cycle is repeated, with orthorhombic geometries interspersed between elongated and compressed tetragonal geometries having symmetry axes permuting between x, y and z, and the electronic wavefunction changing concomitantly. As shown by O'Brien,[39] at this level of approximation, the vibronic wavefunctions are characterized by what are effectively rotational quantum numbers. As ϕ varies cyclically, each ligand undergoes a stretching vibration of very large amplitude, and on a time-averaged basis the complex maintains the regular octahedral geometry of an undistorted complex. However, the ligands move in a concerted manner, so that at any instant of time the complex will have the distorted geometry defined by the particular value taken by ϕ.

In practice, the ideal situation outlined above is never realized, as various effects act to warp the Mexican hat potential surface. Anharmonicity of the ϵ_g vibration, 2nd order electronic effects and configuration interaction with the Cu(II) 4s orbital have all been proposed as warping agents.[37,40] It has been pointed out[37] that the form of the two ϵ_g components may be used to predict the influence of these effects. For Q_θ, the axial ligands move twice as far as the in-plane ligands, whereas for Q_ϵ the ligands move by an equal amount (Fig. 12B). This means that anharmonicity and 2nd order electronic effects will influence only displacements along Q_θ, with the former stabilizing an elongated, and the latter a compressed

tetragonal geometry. Configuration interaction with the Cu(II) 4s orbital occurs with the d_{z^2} (and analogous d_{x^2} and d_{y^2}) components of the electronic part of the wavefunction, and this also maximizes when the displacement is along the Q_θ component, with the greatest stabilization occurring for an elongated geometry. All three effects are generally expected to be comparable in magnitude,[37,40] and as two favor a tetragonal elongation, the overall result is a warping of the potential surface to give three minima at $\phi = 0°$, 120° and 240°, corresponding to the long axis along z, y and x, and three maxima at $\phi = 60°$, 180° and 300° corresponding to tetragonal compressions with the short axes along x, z and y. The relative importance of the factors influencing the warping of the Mexican hat potential surface may vary from one compound to another. For instance, the energy of the 4s orbital is expected to depend upon the effective nuclear charge on the metal, and the anharmonicity of the vibration may be significantly decreased when the complex involves bridging rather than terminal ligands. It is noteworthy that adoption of the Q_θ tetragonal geometry, rather than the Q_ϵ orthorhombic geometry follows the "epikernal" arguments of Ceuleman *et al.*,[14,41] since the former represents a complex of higher symmetry.

For a typical complex such as $Cu(H_2O)_6^{2+}$, simple calculations suggest[37] a warping energy $\beta \approx 300$ cm^{-1}. Thus, although the Jahn–Teller stabilization energy of a 6-coordinate Cu(II) complex is rather high, ~1500 cm^{-1}, the energy difference between the tetragonally elongated and compressed geometries, 2β, is quite low, with orthorhombic geometries lying between these extremes. This means that although a 6-coordinate copper(II) complex is always expected to undergo a large Jahn–Teller distortion, the actual geometry adopted may be strongly influenced by the nature of the ligands or even crystal packing forces, and may sometimes even vary as a function of temperature. As already mentioned, EPR has provided most of the spectroscopic data on the vibronic coupling in 6-coordinate copper complexes, and it is these results which will be covered in the following sections. However, an important exception is the study by Riley *et al.* of the ways in which vibronic coupling influences the absorption[42] and luminescence[43] spectra of the CuF_6^{4-} ion in various lattices.

II.2.(i) Sites of cubic and trigonal symmetry

When the metal–ligand interaction along all six bonds is identical, a potential surface with three equivalent minima is expected. It

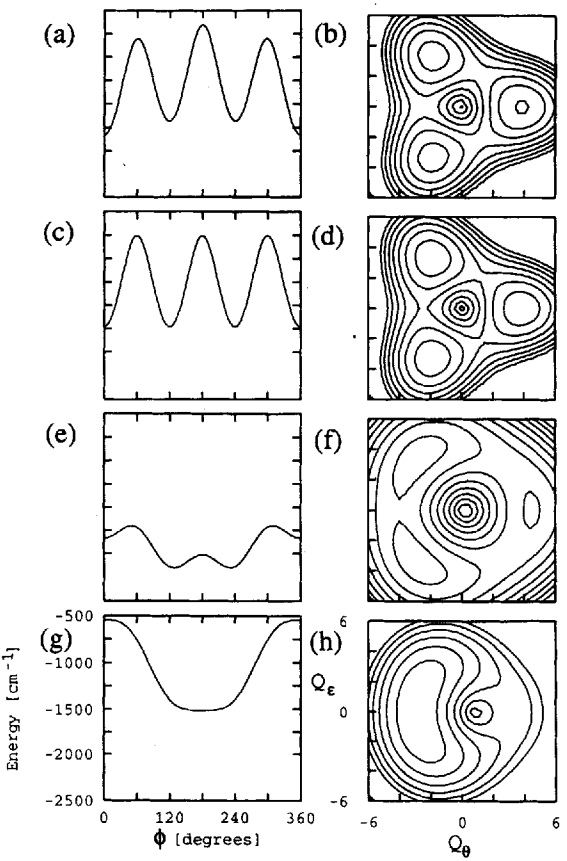

FIGURE 13 Plots of the variation in energy of the minimum of the lower portion of the Mexican hat potential surface as a function of ϕ for the following Cu^{2+} doped compounds: (a) $[Zn(H_2O)_6]GeF_6$, (c) $[Zn(H_2O)_6]SiF_6$, (e) *trans* $Cu(H_2O)_2Cl_4^{2-}$ in NH_4Cl, (g) K_2ZnF_4. The corresponding contour energy plots are shown in (b–h). The contour interval is 100 cm^{-1}, with the outermost contour and the central point of the conical intersection at an energy of zero. The following values of the parameters (in cm^{-1}) were used in the calculations: (a,b) $h\nu$ = 300, V = 900, β = 300, S_θ = 100; (c,d) as for (a,b) but with S_θ = 0; (e,f) $h\nu$ = 210, V = 900, β = 100, S_θ = −200; (g,h) $h\nu$ = 220, V = 675, β = 50, S_θ = −540. See Ref. 56 for details of the method of calculation.

has been shown that in an "ideal" complex of this type with minima at $\phi = 0°$, 120° and 240°, the lowest energy wavefunctions are a vibronic doublet lying slightly lower in energy than a vibronic singlet.[39] These wavefunctions describe tetragonally elongated coordination geometries, and associated electronic functions, but delocalized over the three minima. However, as shown by Ham,[44] in practice small random strains act to make the ligands slightly inequivalent, and this has the effect of localizing the wavefunctions largely in each well. Most experimental work on systems of this type has involved the EPR spectra of Cu^{2+} doped into diamagnetic host lattices of cubic or trigonal symmetry. An important early example was Cu^{2+} doped into $[Zn(H_2O)_6]SiF_6$.[39,45] Here, the metal ion lies on a site of trigonal symmetry, which does not remove the degeneracy of the ^2E_g state of the parent octahedral $Cu(H_2O)_6^{2+}$ complex. At high temperatures, an isotropic EPR signal was observed, but below ~50 K this alters to the anisotropic spectrum characteristic of a tetragonally elongated complex, with the symmetry axis randomly distributed over the three *trans* $Cu-H_2O$ bond directions. The ground state potential surface of a complex of this kind is often shown as a plot of the variation of the energy as a function of ϕ, and a plot of this kind which explains the EPR observations is shown in Fig. 13c. Note that the energy change on moving around the minimum in the potential surface does not follow a strictly circular pathway, since the Jahn-Teller radius of the energy minimum varies slightly as a function of ϕ, as may be seen from the energy contour plot of the lower region of the Mexican hat potential surface in Fig. 13d.

At low temperatures virtually every complex is in one of the three lowest energy states, and the overlap between these wavefunctions is so small that the tunnelling rate is lower than the frequency difference between the EPR signals associated with each level. The observed EPR spectrum is thus a superposition of three spectra, each that of a tetragonally elongated complex with the long axis along a different pair of *trans* $Cu-H_2O$ bonds. At higher temperatures, a significant number of complexes are excited to upper vibronic levels where the wavefunctions are more delocalized. This provides a pathway for exchange between the wells, and when this becomes more rapid than the frequency difference between the EPR signals, an isotropic signal is observed. When Cu^{2+}

is doped into cubic MgO an essentially isotropic EPR signal is observed even at 4.2 K.[46,47] Here it is thought that even the lowest energy wavefunctions overlap sufficiently to allow exchange which is more rapid than the EPR frequency difference. It has been shown that the extent to which the three lowest energy wavefunctions are localized depends upon the relative magnitudes of the barrier height 2β, which decides the energy difference between the vibronic doublet and singlet (the so-called "tunnelling splitting"), and the random strains in the lattice. It is thought that in Cu^{2+} doped MgO the warping of the potential surface is considerably less than that in Cu^{2+} doped $[Zn(H_2O)_6]SiF_6$, and it is this which leads to the difference in the low temperature EPR spectra of the two systems. The form of the slight anisotropy observed in the low temperature spectrum of Cu^{2+} doped MgO suggests that the warping, though small, is similar to that generally observed, i.e., the minima correspond to elongated tetragonal geometries. However, in Cu^{2+} doped CaO the EPR spectra suggest minima at $\phi = 60°$, 180° and 300°, i.e., complexes with *compressed* tetragonal geometries, with the short axes disordered over the three equivalent Cu–O bond directions.[48,49] Here, the low temperature spectra of some samples are close to isotropic,[48] suggesting rapid exchange between the wells, while other samples show the anisotropic spectra expected if exchange between the wells is relatively slow.[49] It appears that in Cu^{2+} doped CaO the random strains in the lattice vary somewhat from one sample to another, and that the delocalization of the lowest wavefunctions produces tunnelling of a rate comparable to the frequency difference between the EPR spectra of the wavefunctions. The fact that a lower warping of the potential surface is observed when Cu^{2+} is doped into MgO and CaO, than into $[Zn(H_2O)_6]SiF_6$, is consistent with the smaller influence expected for the anharmonicity of the ϵ_g vibration in a continuous lattice.[37] It is possible that the unusual stabilization of the tetragonally compressed geometry in the CaO lattice is due to the fact that here the Cu^{2+} substitutes for an ion of significantly larger size—this stereochemistry moves four ligands away from the Cu^{2+} and only two towards it, while the reverse is true for the more common elongated tetragonal arrangement.

II.2.(ii) Sites of tetragonal symmetry

For a centrosymmetric complex where two *trans* ligands are not equivalent to the other four, the Cu^{2+} ion experiences a ligand field "strain" of uniaxial symmetry. When the axial ligands are weaker σ-donors than the in-plane ligands, the strain will reinforce the natural tendency for Cu^{2+} to adopt a tetragonally elongated geometry, stabilizing the minimum in the Mexican hat potential surface which corresponds to the axial elongation lying parallel to the strain direction. When the strain is caused by the presence of two different types of ligand, the stabilization is usually so large that just one type of complex is observed—for instance, a complex such as *trans* $Cu(1,2diaminoethane)_2(NO_3)_2$ exists solely in a form with four short Cu–N and two long Cu–O bonds and the EPR spectrum shows no significant change below room temperature.[50] However, when the ligands are rather similar, as is the case for the complex $Cu(H_2O)_2(HCO_2)_4^{2-}$ formed in Cu^{2+} doped $Ba_2Zn(HCO_2)_6.4H_2O$, the stabilization may be quite small. Here, the EPR spectrum shows a modest temperature dependence, the *g*-values being basically those expected for a complex with a tetragonally elongated geometry and a $d_{x^2-y^2}$ ground state but with the difference between $g_\parallel$ and $g_\perp$ decreasing as the temperature is raised.[51] Similar behavior is observed[52] for Cu^{2+} doped $[Zn(H_2O)_6]GeF_6$, with lattice forces here acting to stabilize the form with two metal–ligand bonds longer than the other four. At low temperature the EPR spectrum corresponds to just this form. However, as the temperature is raised, the vibronic levels corresponding to complexes with long bonds to the other four water molecules become thermally populated, and as the exchange rate is faster than the difference between the EPR signals measured in frequency units, the *g*-values converge towards an isotropic value at high temperature. The temperature dependence of the *g*-values of this complex is shown in Fig. 14a, and the ground state potential surface consistent with this data in Figs. 13a and 13b.

A more interesting situation results when the uniaxial strain acts to *oppose* the natural tendency of Cu^{2+} to adopt a tetragonally elongated geometry, i.e., when two *trans* ligands produce a stronger σ-perturbation than the other four. When the strain is very large,

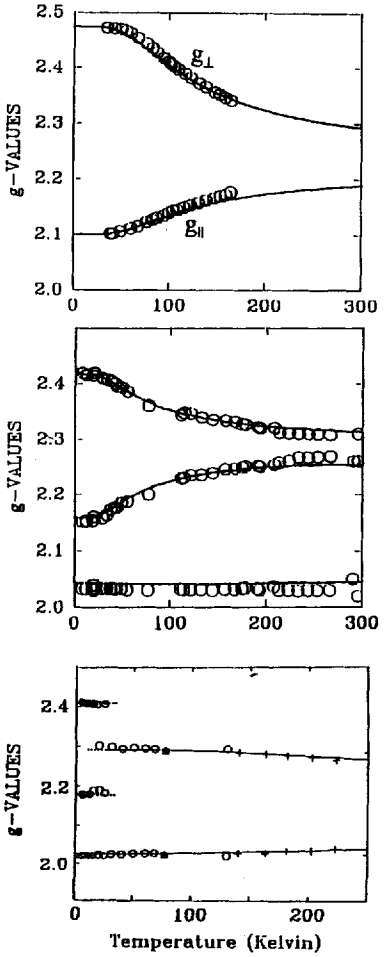

FIGURE 14 Experimental and calculated g-values (circles and lines) for (a) Cu^{2+} doped $[Zn(H_2O)_6]GeF_6$; (b) Cu^{2+} doped $K_2[Zn(H_2O)_6](SO_4)_2$; (c) *trans* $Cu(H_2O)_2Cl_4^{2-}$ in Cu^{2+} doped NH_4Cl. See text for references to the data and method of calculation.

it will "force" the unusual tetragonally compressed geometry, which is what occurs, for instance, in the complex $Cu(NH_3)_2Cl_4^{2-}$.[53] However, as pointed out by Reinen *et al.*,[54,55] when the strain is small, its effect is to produce two equivalent minima in the potential

surface, each corresponding to an orthorhombic ligand geometry. The strain direction is conventionally taken as z, so that it acts to stabilize the geometry and concomitant electronic structure corresponding to $\phi = 180°$, one of the three equivalent saddlepoints on the strain-free Mexican hat potential surface (Figs. 13c and 13d). As the strain increases in magnitude, the minima which occur at $\phi = 120°$ and 240° in the strain-free surface progressively move towards 180°, and become lower in energy than that at 0°. This effect is illustrated by the potential surfaces shown in Figs. 13e and 13f. When the strain reaches $\sim 9\beta$ in magnitude, the two minima coalesce to produce a single, shallow well centered at 180° (Figs. 13g and 13h).

A potential surface similar to that in Figs. 13e and 13f is thought to occur for the complex *trans* $Cu(H_2O)_2Cl_4^{2-}$ formed when Cu^{2+} is doped into NH_4Cl at low pH.[56] The variation of the molecular g-values of this complex as a function of temperature is shown in Fig. 14c. Above ~40 K the g-tensor shows tetragonal symmetry with $g_{\parallel} < g_{\perp}$, a characteristic normally associated with a ground state wavefunction having the unpaired electron in the d_{z^2} orbital and a tetragonally compressed ligand coordination geometry. Below this temperature, the EPR signal responsible for $g_{\perp}$ splits into two, and the g-tensor assumes orthorhombic symmetry. This can be explained if the ratio of the strain to the warping parameter, S_θ/β, ≈ -2, producing two equivalent minima in the potential surface. Each of these corresponds to an orthorhombic coordination geometry with short bonds to H_2O, and intermediate and long bonds to Cl^-, but with the directions of the intermediate and long bonds interchanged in the two wells. If the strain experienced by each Cu^{2+} were of strict D_{4h} symmetry, the lowest wavefunction would be a pair of closely spaced vibronic singlets delocalized over the two wells. In practice, however, small random strains due to lattice defects lower the symmetry, making the two minima slightly inequivalent, and causing the wavefunction of one singlet to become localized largely in the well at ~120°, and the other in that at ~240°. Above ~40 K the thermal population of higher, more delocalized vibronic levels allows exchange between the lowest wavefunctions which is more rapid than the frequency difference between their EPR signals, so that an averaged spectrum is observed. Below ~40 K, only the lowest pair of wavefunctions is

significantly populated, and these are sufficiently localized that the tunnelling rate is slower than the EPR frequency difference, so that the spectrum of each level is resolved (because the random strains are so small the g-tensors differ only in the relative orientation of the principal axes of the two higher g-values). The axial strain in the complex was estimated as $S_\theta \approx -200\ cm^{-1}$, with the warping parameter $\beta \approx 100\ cm^{-1}$. The strain here represents the stronger σ-donor effect of the H_2O ligand compared with Cl^-, the value agreeing with estimates obtained by analysis of the *d-d* spectra of copper(II) chloride and hydrate complexes.[56]

When the strain reaches $\sim 9\beta$, it becomes just sufficient to produce a single minimum at $\phi = 180°$ in the Mexican hat potential surface. A complex described by such a surface thus has a tetragonally compressed coordination geometry with the short metal–ligand bonds parallel to the strain direction. As pointed out by O'Brien,[39] the form of the potential is such that the complex may be thought of as undergoing "angular" vibrations, and since the minimum occurs along the Q_θ component of the e_g mode, the angular vibrations involve displacements in the Q_ϵ component of this mode. The electronic component of the vibronic wavefunction corresponding to $\phi = 180°$ is d_{z^2}, but vibronic coupling with the angular vibration introduces a $d_{x^2-y^2}$ component into each energy level. To first order, the effect is analogous to the mechanism whereby intensity is induced into a parity forbidden electronic transition (see Section II.1.(i)a). Rather than admixing an *ungerade* into a *gerade* electronic state, the angular vibration admixes the $d_{x^2-y^2}$ component of the wavefunction associated with the upper portion of the Mexican hat potential surface at the $\phi = 180°$ geometry into the wavefunction of the lower surface. Assuming that to a first approximation the angular vibration corresponds to simple harmonic motion, it may be shown[11] that its mean-square amplitude is proportional to $(2v + 1)/h\nu$, where $h\nu$ is the energy of the vibration and v is the vibrational quantum number. If the warping parameter β is small, the angular vibration may be quite low in energy. This means that not only will the lowest energy $v = 0$ level be significantly contaminated by $d_{x^2-y^2}$ due to the zero-point motion of the ligands, but a significant change in the weighted average of the wavefunctions will occur between 0 K and 300 K because of the close spacing of the energy levels. It has been

suggested[11] that such a situation occurs for the CuF_6^{4-} complex formed when Cu^{2+} is doped into K_2ZnF_4. Here, a significant $g_{\parallel}$ shift from the value expected for a pure d_{z^2} ground state is observed, even close to 0 K, and the g-values are significantly temperature dependent (Fig. 15). The g-values expected in the absence of vibronic coupling are indicated by arrows, the slight deviation

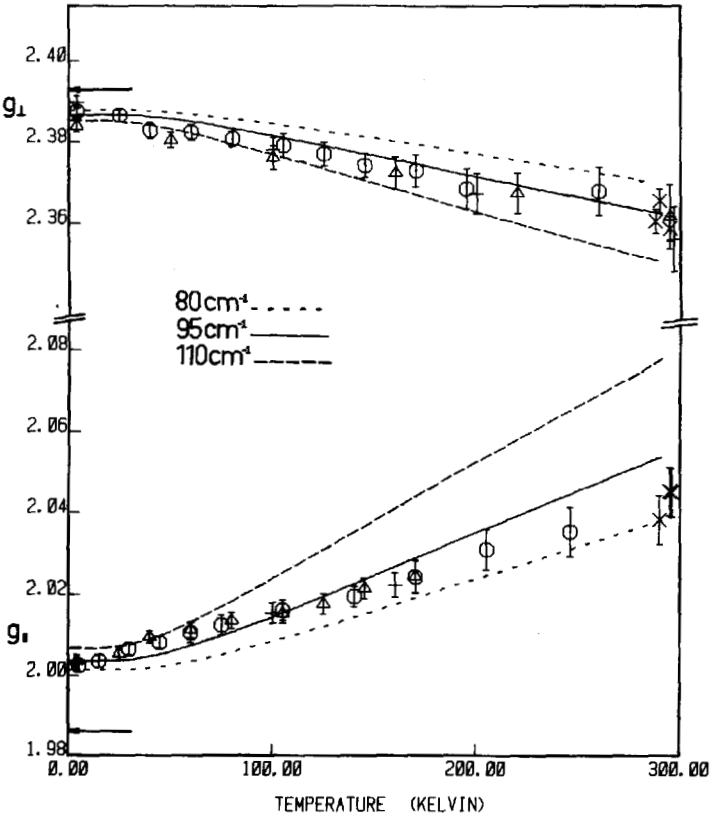

FIGURE 15 Temperature dependence of the g-values of Cu^{2+} doped K_2ZnF_4; the uncertainties are indicated by error bars, and data from different samples are shown using individual symbols. The g-values expected in the absence of vibronic coupling are indicated by arrows, and the curves show the values calculated assuming coupling with harmonic "angular" vibrations of 80, 95 and 110 cm^{-1}; see text for the method of calculation.

of g_z from the free electron value of 2.0023 being due to 2nd order spin-orbit effects. Calculations based on this model of simple vibronic coupling showed that both the g-shifts at low temperature and the temperature dependence of the g-values are reproduced quite well assuming an energy of the angular vibration of ~95 cm^{-1}.[11] Here the g-shifts were calculated by including spin-orbit coupling using perturbation theory to second-order and assuming simple Boltzmann statistics over the energy levels. The fact that the EPR peaks vary smoothly in position as the temperature is changed implies that the exchange between the vibronic energy levels is more rapid than the frequency difference between the signal associated with each level. The proportion of $d_{x^2-y^2}$ in the lowest energy $v = 0$ vibrational level was estimated to be ~3%, but this rises to ~9% and 15% for the $v = 2$ and 3 levels, and the low energy of the vibration means that these are significantly populated at room temperature. An improved data fit was obtained by a more exact calculation where the vibronic wavefunctions were estimated by applying linear Jahn–Teller coupling, plus higher-order warping and the uniaxial strain, to a basis set of the d_{z^2} and $d_{x^2-y^2}$ electronic wavefunctions plus ~40 levels of the ϵ_g vibration. This gave values for the strain of $S_\theta \approx -540\ cm^{-1}$ and the warping parameter $\beta \approx 50\ cm^{-1}$.[11]

It thus seems that the significant effects due to vibronic coupling in Cu^{2+} doped K_2ZnF_4 are due to the low inherent warping of the Mexican hat potential surface, combined with the fact that the axial compression of the ligand field is only just sufficient to stabilize the tetragonally compressed coordination geometry. In the similar CuF_6^{4-} complex present in Cu^{2+} doped Ba_2ZnF_6, the shift in $g_\parallel$ from the value expected in the absence of vibronic coupling and the temperature dependence of the g-values are much smaller ($g_\parallel = 1.99_2$ at 4.2 K, rising to 2.00_2 at 300 K) and the data can be reproduced by similar calculations assuming a strain of $S_\theta \approx -1000\ cm^{-1}$ and warping parameter $\beta \approx 80\ cm^{-1}$.[57] The higher value of the strain in the latter compound is consistent with the structures of the two host lattices. In K_2ZnF_4 all six Zn–F bond lengths are equal within experimental error,[58] so that the strain is due solely to the fact that the axial fuorides are terminal ligands, while the in-plane fluorides bridge to Zn^{2+} ions. The type of coordination is identical in Ba_2ZnF_6, but here the axial Zn–F bonds are sig-

nificantly shorter than the in-plane ones,[59] suggesting an increased axial compression to the ligand field due to lattice forces. Vibronic coupling effects are also rather small for the complex *trans* $Cu(NH_3)_2Cl_4^{2-}$ formed when Cu^{2+} is doped into NH_4Cl at high pH.[56] Here the g-values at 4.2 K $g_\parallel = 1.996$, $g_\perp = 2.220$ change only slightly on warming to 298 K ($g_\parallel = 2.0095$ and $g_\perp = 2.209$) and the data can be reproduced by an axial strain of $\sim -1200\ cm^{-1}$ and a warping parameter $\beta \approx 100\ cm^{-1}$.[56] The much higher value of the strain compared with the analogous complex *trans* $Cu(H_2O)_2Cl_4^{2-}$ ($\sim -200\ cm^{-1}$) is consistent with the fact that NH_3 is a significantly stronger σ-donor than H_2O.

II.2.(iii) Sites of orthorhombic symmetry

As mentioned in the two preceding sections, even when the overall symmetry at the Cu^{2+} ion in a crystal is cubic or tetragonal, small random strains lower the symmetry of the ligand field of any particular metal ion to orthorhombic. The energy shifts caused by these random strains are very small, less than $\sim 2\ cm^{-1}$,[46] so that they do not influence the population differences of the energy levels at normally accessible temperatures. However, they have the important effect of localizing the lowest energy vibronic wavefunctions in different potential energy minima, where these would otherwise be delocalized if the minima were truly symmetry equivalent. When the crystallographic symmetry at the Cu^{2+} is less than tetragonal, the orthorhombic component to the strain will usually be quite large, sometimes comparable to thermal energies, and this may cause quite different effects to be observed.

The earliest example of a system of this kind to be studied in detail was Cu^{2+} doped into $K_2[Zn(H_2O)_6](SO_4)_2$. Here, Silver and Getz observed[60] that while at 4.2 K the g-values are those expected for a Cu^{2+} complex with a tetragonally elongated geometry with a slight orthorhombic distortion, as the temperature increases to 300 K, the upper two g-values converge towards their mean value (Fig. 14b). This was explained in terms of a warped Mexican hat potential surface with three strongly localized minima, the wavefunction associated with each corresponding essentially to a tetragonally elongated octahedron with the long axis along three different directions in the lattice, and with the energy of each minimum

differing because of the orthorhombic strain. At 4.2 K effectively all the complexes occupy the lowest energy level, and the observed g-tensor is just that of this complex. On raising the temperature, a significant number of Cu^{2+} ions are excited to the level localized in the second well $\sim 75\ cm^{-1}$ higher in energy. The geometry and electronic wavefunction of this level are similar to that of the lowest level, except for the interchange of the long and intermediate Cu–O bond directions and concomitant electronic wavefunction lobes. As the rate of exchange between these two "conformational isomers" is more rapid than the frequency difference between their EPR signals, the g-values are the population weighted average of the two levels, and gradually approach their mean as the Boltzmann population of the upper level approaches that of the lower level at high temperatures. The level localized in the third well is much higher in energy, and is thus not significantly populated at 300 K, so that the third g-value is unaffected by temperature.

The basic correctness of the Silver and Getz model was confirmed in a detailed study[38] by Riley *et al.* in which the vibronic wavefunctions, calculated by applying an orthorhombic lattice strain plus linear and 2nd order Jahn–Teller coupling to an appropriate basis set of E_g electronic and ϵ_g vibrational wavefunctions, were used to estimate the temperature dependence of the g-values (Fig. 14b). A contour map of the lower Mexican hat potential surface calculated in this way is shown in Fig. 16a, and schematic plots of the vibrational and electronic probability functions for the four lowest levels are also given, together with the orientations of the wavefunctions. The potential surface has three distinct minima, the two lower being separated in energy by $\sim 70\ cm^{-1}$, and the third some $1000\ cm^{-1}$ higher in energy. The two lowest vibronic wavefunctions are both quite strongly localized, one in each of the lower energy wells, and the energy separation between these, 72 cm^{-1}, agrees well with that of the Silver–Getz model, $\sim 75\ cm^{-1}$. With the principal strain axis acting as a compression along z, and the orthorhombic component acting as a compression along y, the electronic part of the lowest energy wavefunction corresponds largely to $d_{z^2-y^2}$, while that of the second lowest corresponds largely to $d_{z^2-x^2}$; the corresponding plots for the 3rd and 4th levels indicate increasing delocalization of the lobes over all three Cartesian axes (Fig. 16b). This study also considered data for Cu^{2+} doped into

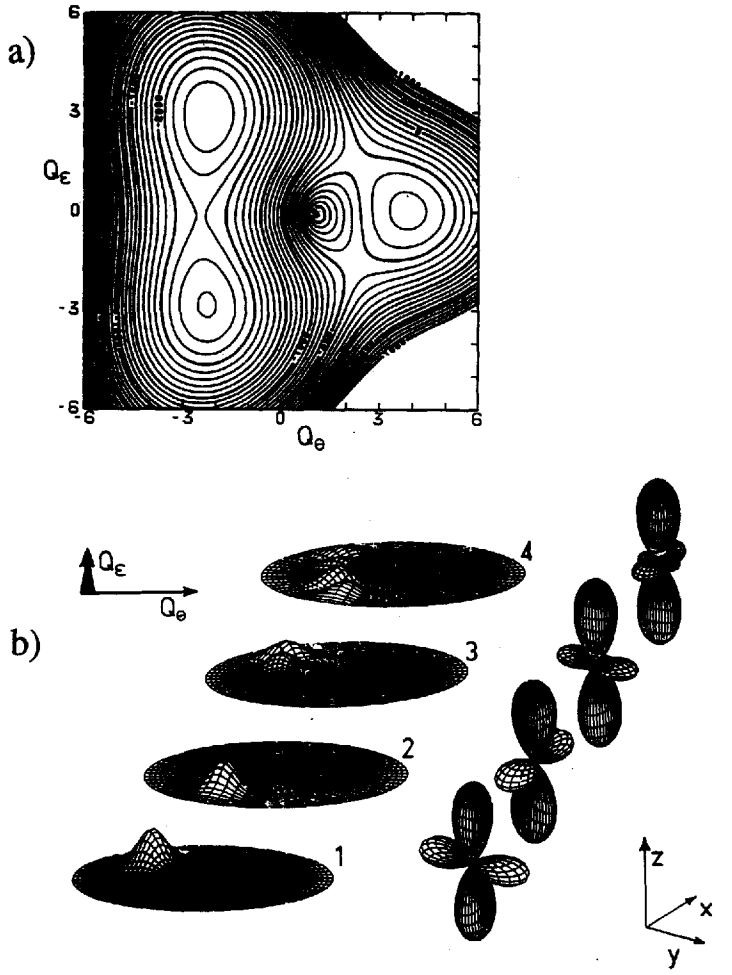

FIGURE 16 (a) Energy contour plot of the lower portion of the Mexican hat potential surface of the $Cu(H_2O)_6^{2+}$ ion in Cu^{2+} doped $K_2[Zn(H_2O)_6](SO_4)_2$. (b) The probability plots of the vibrational and electronic parts of the four lowest energy levels are shown on the left and right, respectively; the axes in the Q_θ, Q_ε vibrational and x, y, z molecular coordinate systems are shown. The following parameters (in cm^{-1}) were used in the calculations: $h\nu = 300$, $V = 900$, $\beta = 300$, $S_\theta = -1000$, $S_\varepsilon = 55$.

Zn^{2+} Tutton salts with other counter-cations. While a generally similar pattern was found, the energy difference between the two lower energy wells was found to increase along the series $K^+ < Rb^+ < NH_4^+ < Cs^+$ and agreement with the simple Silver–Getz model became progressively poorer. Thus, for the NH_4^+ salt, the former model suggested an energy separation of ~230 cm^{-1} between the "conformational isomers," while the more detailed study suggested that the vibronic wavefunction localized largely in the second well was 181 cm^{-1} higher in energy than the ground vibronic level. For the Cs^+ salt, where the Silver–Getz treatment yields an energy of ~290 cm^{-1} for the upper level, the more complete study yielded a pair of closely spaced levels at 292 and 293 cm^{-1}, both delocalized over the two wells.

It was concluded[38] that the Silver–Getz model will be a good approximation when the inherent warping of the Mexican hat potential surface in favor of the tetragonally elongated coordination geometry is significantly larger than the energy separation between the wells. In the above study, β for the $Cu(H_2O)_6^{2+}$ ion was estimated to be ~300 cm^{-1}, and the orthorhombic component of the strain as ~55 cm^{-1} and ~200 cm^{-1} for the K^+ and Cs^+ host lattices, respectively. The corresponding axial components of the strain were estimated to be -1000 cm^{-1} and -650 cm^{-1} for these two salts, these largely deciding the energy of the third well, and the positions of the minima in the Mexican hat surface in each host lattice. The axial strain values represent strong compressions to the ligand field, and it is only the high value of β that maintains basically tetragonally elongated tetragonal coordination geometries in this series of hydrates. As already mentioned, the axial compression needs to be greater than ~9β in order to stabilize a compressed tetragonal geometry, otherwise the compression merely shifts two of the minima corresponding to tetragonal geometries to ones representing orthorhombic geometries. In these compounds, the asymmetry in the ligand field is caused by lattice forces, which should also influence the bond lengths in the host lattice. The axial and orthorhombic strain values estimated from the EPR of Cu^{2+} doped $K_2[Zn(H_2O)_6](SO_4)_2$ imply changes of ~ -5.1, 2.3 and 2.8 pm in the Zn–O bond lengths along z, y and x. These compare favorably with the deviations of $-6.5(0.4)$, 2.9(0.5)

and 3.6(0.5) pm observed by X-ray crystallography,[61] the standard deviations being shown in parentheses.

With the above qualifications, the Silver–Getz model thus provides a realistic and relatively simple method of interpreting the temperature dependence of the EPR spectra of orthorhombic Cu^{2+} complexes, and it has been applied in this way for a range of compounds.[62] EPR spectroscopy focuses on changes in the electronic components of the vibronic wavefunctions, but concomitant changes occur in the vibrational parts of the wavefunctions, and for a pure Cu^{2+} compound these may be observed by determining the crystal structure at different temperatures. Several studies of this kind have been undertaken,[63] the most detailed being those by Simmons *et al.*,[64,65] and much of the data have been discussed by Bürgi.[66] Particular attention has been paid to complexes of the form $[Cu(diamine)_2(O_2X)]Y$, where diamine is a chelating aromatic amine, O_2X is a chelating oxy-anion and Y is a counter-anion. In early studies, the data were interpreted using a model involving so-called pseudo-Jahn–Teller coupling.[64] Here, the wavefunction corresponding to the tetragonally compressed coordination geometry favored by the axial compression to the ligand field is perturbed by vibronic coupling with the upper component of the parent ^2E_g state, where the wavefunction corresponds to the elongated coordination geometry. This approach, which was also used by Sorokin and Cherkin[67] to interpret the EPR spectrum of the complex $Cu(NH_3)_2Br_4^{2-}$ formed by doping Cu^{2+} into NH_4Br at high pH, produces a potential surface similar to that obtained by adding a "strain" to the Jahn–Teller warped Mexican hat potential surface. It has sometimes been suggested[68] that application of the Jahn–Teller effect to complexes involving a set of inequivalent ligands is inappropriate, as this theorem does not strictly apply once the electronic degeneracy is removed by low symmetry components of the ligand field. In fact, provided that the "strain" caused by the ligand inequivalence is significantly less than the effect of the linear Jahn–Teller coupling, as will generally be the case for octahedral Cu^{2+} complexes, the two approaches are essentially equivalent. The advantage of an approach based upon conventional Jahn–Teller coupling is that it builds upon a widely used model, and experimental values are available for most of the parameters used in the calculations, and later studies of the tem-

perature dependence of the crystal structures of the above Cu^{2+} compounds have used the Jahn–Teller based approach.[65]

The basic "strain" in the $[Cu(diamine)_2(O_2X)]^+$ complexes is caused by the fact that the pair of *trans* amine nitrogen atoms produces a stronger σ-perturbation than the two pairs of *trans* oxygen and nitrogen ligands. The strain is insufficient to stabilize a compressed tetragonal geometry, but causes two equivalent minima in the Mexican hat potential surface (see preceding section, Figs. 13e and 13f). Usually, crystal lattice forces produce an orthorhombic component to the strain which renders these minima slightly inequivalent, causing a potential surface similar to that of the $Cu(H_2O)_6^{2+}$ complexes in the Cu^{2+} doped zinc Tutton salts (Fig. 16b). At low temperature, only the level localized in the lowest well is populated, and the crystal structures thus show the geometry associated with this wavefunction, with long bonds to one oxygen atom of the chelating oxy-anion and the amine nitrogen *trans* to it, intermediate bonds to the other oxygen and *trans* amine nitrogen, and short bonds to the pair of *trans* amine nitrogen atoms. As the temperature is raised, the vibronic level largely localized in the second well becomes thermally populated, and the observed crystal structure is then the superposition of the structures associated with each well, weighted by their Boltzmann populations. Sometimes, the atomic positions of the complexes associated with each well can be resolved, and within experimental uncertainty these are identical except for the interchange of the directions of the long and intermediate bonds, as assumed in the Silver–Getz model.[65] However, generally this is not the case, and as the temperature rises it is simply observed that the apparent positions of the ligand atoms associated with the longest bonds move closer to the Cu^{2+}, while those of the ligand atoms associated with the intermediate bonds move away. In addition, the thermal ellipsoids of this set of atoms become greatly elongated along the bond directions. The effect is more pronounced for the oxygen atoms, suggesting that most of the motion involves the chelating oxy-anion. This may be seen from the *ORTEP* plots of the copper and in-plane ligand donor atoms obtained from the crystal structures of $[Cu(phen)_2(O_2CCH_3)]ClO_4$, phen = 1,10-phenanthroline, at various temperatures (Fig. 17).[65]

To interpret the temperature dependence of the structures quan-

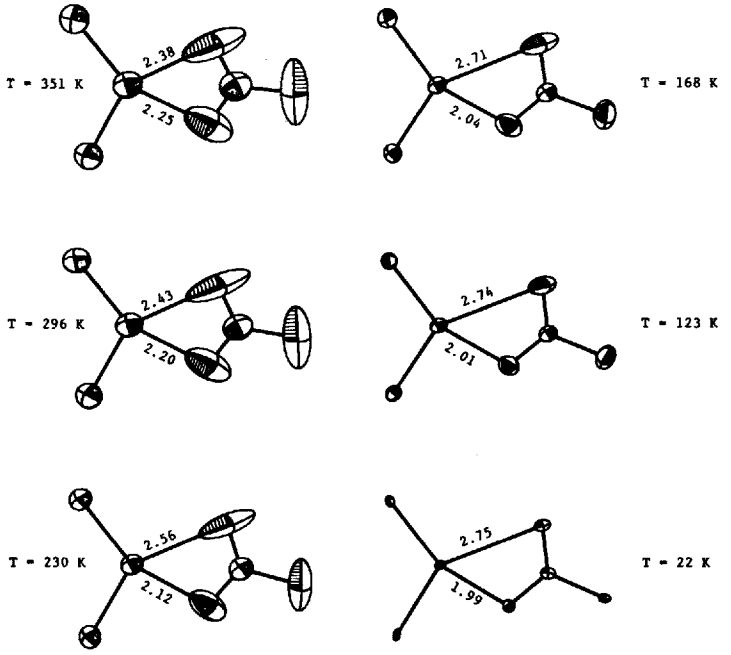

FIGURE 17 *ORTEP* plots of the equatorial atoms in $[Cu(phen)_2(O_2CCH_3)]ClO_4$ at different temperatures. All are drawn to the same scale with the CuO_2 groups in the plane of the page; Cu–O bond distances are also indicated. Data from Ref. 65.

titatively, the low temperature X-ray determination is used to establish the basic structure of the complex associated with the lowest minimum, and an identical geometry is assumed for the complex associated with the upper well, except for the interchange of the intermediate and long metal–ligand bond directions. The apparent ligand positions at higher temperatures are then used to deduce the fraction of the complex occupying each energy level. If the ratio of the number of complexes in the upper level to that in the lower level at any temperature T is K and the simple Silver–Getz approach holds, a plot of $\ln(K)$ against $1/T$ should follow a straight line passing through the origin, and this was indeed found to be the case for the compound $[Cu(bipy)_2(O_2N)]NO_3$, bipy = 2,2′-bipyridyl,[64] with an energy difference between the structural con-

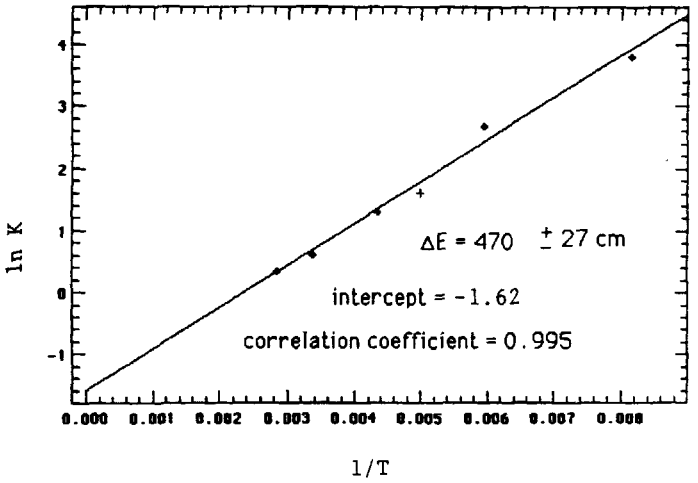

FIGURE 18 Linear least-squares plot of $\ln(K)$ against $1/T$, where K is the ratio of complexes in the upper to the lower energy state, for $[Cu(phen)_2(O_2CCH_3)]ClO_4$. Data from Ref. 65.

formers of 91 ± 15 cm^{-1}. A good straight line plot is also obtained for $[Cu(phen)_2(O_2CCH_3)]ClO_4$ (Fig. 18), the slope suggesting an energy separation of 470 ± 27 cm^{-1} for this compound. Here, however, the line of best fit no longer passes through the origin. Similar deviations occur for other compounds in which a relatively large energy difference occurs between the structural "isomers". It was suggested[65] that the deviation may be due to delocalization of the wavefunctions associated with the upper well. While this seems plausible, as the detailed analysis of the EPR data of Cu^{2+} doped into various zinc Tutton salts suggested that for this reason the Silver–Getz approach becomes less realistic as the energy of the upper well increases,[38] it is also possible that coupling with internal ligand vibrations may influence the behavior of the $[Cu(diamine)_2(O_2X)]^+$ complexes. In addition, the properties of pure Cu^{2+} compounds may be modified by cooperative interactions. These will occur when the change of geometry of one complex influences the potential surfaces of its neighbors. Simple Boltzmann statistics will then no longer apply, as the average potential surface will become temperature dependent. For these reasons, while the Silver–Getz model seems to provide a good general

picture of the temperature dependence of the crystal structures of copper compounds, interpretations of the fine details must be viewed with caution.

III. SUMMARY AND DIRECTIONS FOR FUTURE RESEARCH

A common feature of 4- and 6-coordinate copper(II) complexes is the fact that the stereochemistry is dominated by Jahn–Teller vibronic coupling. However, the nature of the interaction differs for the two coordination numbers in several important respects. Distortion away from the tetrahedral geometry occurs via a bending mode, while the octahedral geometry is rendered unstable by a stretching vibration. In the former case, the force constant is therefore generally quite small, and as the d-orbitals in a tetrahedral complex are only weakly antibonding, the Jahn–Teller coupling coefficient is also quite modest. Since the size of the distortion is decided by the balance between these two parameters, this can be strongly influenced by factors such as lattice interactions. A wide range of angular distortions is thus observed for 4-coordinate copper(II) complexes, with this extending as far as the limiting planar ligand arrangement. For 6-coordinate complexes, on the other hand, the force constant of the active vibration and the Jahn–Teller coupling constant are both relatively large, so that the overall distortion tends to fall within a rather narrow range. However, whereas for tetrahedral copper(II) complexes distortion always occurs in one direction—towards the planar geometry—for 6-coordinate complexes distortion can produce either a tetragonally elongated or compressed octahedron, and these have quite different electronic ground states. Moreover, the Jahn–Teller active vibration is doubly degenerate, and distortion along the second component of the mode provides a low energy pathway between the two tetragonal geometries. This means that although the energy stabilization associated with the overall distortion of a 6-coordinate copper(II) complex is quite large, the actual geometry may be influenced by quite small perturbations. Moreover, in contrast to 4-coordination, where the ground electronic state remains basically similar over the whole range of distortions, for 6-coordinate com-

plexes the electronic wavefunction depends upon the component of the vibration along which distortion occurs.

For planar complexes, the very low energy of the out-of-plane bending mode corresponding to the Jahn–Teller active vibration of the parent tetrahedral geometry is responsible for the large temperature dependence of the intensities of the *d-d* transitions. In the case of planar $CuCl_4^{2-}$, it has been suggested that the significant shifts to lower energy of the band maxima which occur on warming from 10 K to 300 K, and the anomalous vibrational fine structure observed in the low temperature spectra of certain compounds, are both caused by the fact that the equilibrium geometry shifts towards a tetrahedron in the excited states. This hypothesis could be tested more directly if the luminescence of the complex could be observed, which might be feasible, particularly if it were doped into a suitable host lattice such as K_2PtCl_4. The nature of the vibrational fine structure observed in the low temperature optical spectra, and to a lesser extent the shifts in the band maxima of compounds containing planar $CuCl_4^{2-}$, are very sensitive to the nature of the counter-cation. It has been proposed[31] that this may be due to the influence of the cation on the form of the excited state potential surfaces. It would be interesting to observe the effect of high pressure on these aspects of the electronic spectra, as this should perturb the cation–anion interactions.

For copper (II) complexes with six identical ligands, distortion almost always occurs along the vibrational component producing a tetragonally elongated geometry, with the unpaired electron occupying the $d_{x^2-y^2}$ orbital. However, the corresponding compressed tetragonal geometry, with the unpaired electron in d_{z^2}, is only a few hundred cm^{-1} higher in energy, and this may be reached smoothly by motion of the ligands along the second component of the mode, which produces an orthorhombic ligand arrangement. The long bonds may occur to any of the three pairs of *trans* ligand atoms, and Cu^{2+} complexes sometimes crystallize with two or more orientations disordered in the crystal lattice. This may lead to problems in determining the geometry of the complex, and indeed raises the question of how this is best defined. Data reported recently[69] for the centrosymmetric $CuCl_6^{4-}$ ion in (3-chloroanilinium)$_8$[$CuCl_6$]Cl_4 illustrate this point. The crystal structure at 300 K shows two short and four long Cu–Cl bonds, suggesting the

unusual tetragonally compressed geometry, with the unpaired electron in d_{z^2}. The form of the molecular g-tensor, $g_{\parallel} = 2.04$, $g_{\perp} = 2.20$, with the former parallel to the short Cu–Cl bonds, conforms to this hypothesis, though the significant $g_{\parallel}$-shift from the free electron value argues against a d_{z^2} ground state (see Section I.1). It was suggested that the anomalous $g_{\parallel}$-shift is due to vibronic admixture of $d_{x^2-y^2}$ into the ground state, and the significant elongation of the thermal ellipsoids of the more distantly bound Cl^- ions along the bond directions was taken to support this hypothesis. If this were correct, the $g_{\parallel}$-shift should decrease significantly on cooling, and subsequent measurements[70] showed that this does not occur. This evidence, combined with analysis of the polarization behavior of the electronic transitions, led to a second hypothesis,[70] that at the local level the complex has a tetragonally elongated geometry, with a small orthorhombic distortion, but with the long and one pair of short Cu–Cl bonds disordered to give the *appearance* of four bonds of intermediate length. This second hypothesis was confirmed by analysis of the *EXAFS* (extended X-ray absorption fine structure) of the compound,[71] with the positions of the chlorides agreeing well with an analysis of the thermal ellipsoids determined in the X-ray analysis in terms of a statistical disorder of long and short bonds, rather than a low energy vibration. Because it provides information on the local coordination geometry, rather than the average position of the atoms in a crystal lattice, *EXAFS* provides a powerful way of investigating stereochemistry in compounds where disorder may be present, and should be used increasingly as the technique becomes more widely available. The determination of crystal structures at low temperature will also help resolve ambiguities of this kind, both by increasing the chance that the disordered atoms may be resolved, and because comparison of the thermal ellipsoids of atoms at high and low temperature should allow vibrational effects to be distinguished from disorder, as the latter will not be temperature dependent (unless the two sites differ in energy). The above results also illustrate the importance of investigating the temperature dependence of EPR spectra whenever vibronic coupling may influence the ground state, and the fact that when exchange between two forms of a complex is more rapid than the frequency difference between their EPR signals, as occurs for the present compound

even at very low temperature, an average spectrum will be observed.

In the above example the average ligand positions, and the symmetry of the *g*-tensor both suggest a complex with a tetragonally compressed geometry, so it is pertinent to ask in what sense this is incorrect. A key point which is represented wrongly in this picture is the form of the metal–ligand interactions which decide the electronic wavefunctions of the complex. The Franck–Condon principle suggests that these are decided by the most probable ligand positions at any instant of time. In the present example, this is the tetragonally elongated geometry, and any interpretation of the electronic spectrum using the space- and/or time-averaged tetragonally compressed geometry is erroneous. Similarly, the discussion of the magnetic behavior in terms of interactions between a set of identical complexes with the unpaired electron occupying the d_{z^2} orbital is invalid, and must be replaced by a more complicated picture involving tetragonally elongated complexes with the unpaired electron in $d_{z^2-y^2}$ type orbitals, and the direction of the long axes disordered throughout the lattice. Clearly, whenever a copper(II) complex appears to adopt a geometry in which the Jahn–Teller distortion is absent, or takes an unusual form, it is most important to verify that this indeed represents the local coordination geometry.

The above example represents a situation in which the 6-ligands are rendered inequivalent by lattice forces, and such an effect is represented in the theoretical models developed by physicists by the addition of a "strain" parameter to the Jahn–Teller coupling. When the strain is caused by asymmetry in the field produced by different ligands, inorganic chemists will often be able to use optical and/or EPR spectroscopy to supply a numerical estimate for the parameter, and this should make the prediction of compounds with novel properties easier. Unusual behavior tends to be observed when a uniaxial strain acts to oppose the natural tendency of copper(II) to adopt a tetragonally elongated geometry, i.e., when one pair of *trans*-ligands are stronger σ-donors than the other four ligands. If the difference is large, the uncommon tetragonally compressed geometry may result, but a modest compression produces two equivalent orthorhombic geometries.

When the site symmetry at the Cu^{2+} in a complex is ortho-

rhombic, the states corresponding to an elongation along each pair of trans Cu–ligand bond directions are rendered energetically inequivalent by the anisotropy of the interactions with the surrounding lattice. Sometimes the two lower energy states are both thermally accessible, and the time-averaged vibronic wavefunction is then temperature dependent. Changes in the electronic component are conveniently studied by EPR spectroscopy, while those in the vibrational part are observed by measuring the crystal structure at different temperatures. So far, the EPR studies have been limited to complexes formed when Cu^{2+} is doped into diamagnetic host lattices, and a relatively sophisticated model has been developed to interpret the data.[11,38,56,57] An important extension of the model will be to see whether EPR and structural data obtained concurrently on pure compounds can be interpreted satisfactorily. Preliminary results suggest that this is indeed feasible,[72] and this is important as it provides a way of quantifying the anisotropy of the "strain" due to the surrounding lattice. An example of the type of study which this approach allows is provided by the compound $(NH_4)_2[Cu(H_2O)_6](SO_4)_2$. Here, both EPR studies and crystal structure determinations imply[73] that the orthorhombic $Cu(H_2O)_6^{2+}$ complex undergoes a temperature dependent equilibrium between two forms in which the directions of the long and intermediate Cu–O bonds interchange. This may be explained if the surrounding lattice produces a significant axial compression, combined with a small orthorhombic perturbation, at the Cu^{2+}. Of particular interest is the fact that the corresponding deuterated compound exhibits similar behavior, but with the directions of the long and intermediate Cu–O bonds reversed.[74] The model explains this behavior essentially in terms of a change in sign of the small rhombic component of the lattice "strain." Moreover, on increasing the pressure to ~1.5 kbar, the deuterated compound switches to the structure of the hydrogenous compound,[75] suggesting that the strain is pressure dependent. This appears to be the only known example of a relatively large structural change associated with isotopic substitution. Although no detailed explanation for this behavior has been proposed yet, it seems likely that it is rooted in the vibronic coupling mechanism which causes the distorted geometry of copper(II) complexes. Because the mass of the ligand influences the energy of a metal–ligand vibration, the Jahn–Teller radius of

the deuterated complex is slightly larger than that of the hydrogenous. It seems likely that crystal packing forces discriminate between the two complexes on this basis, a fitting illustration of the all-pervading influence of vibronic coupling upon the chemistry of copper(II).

Acknowledgment

Dr. Mark J. Riley is thanked for many fruitful discussions and for help with preparation of several figures.

References

1. H. A. Jahn and E. Teller, Proc. Roy. Soc. A **161**, 220 (1937).
2. C. E. Schäffer, Struct. Bond. **5**, 68 (1968).
3. D. Smith, Struct. Bond. **12**, 49 (1972).
4. M. Bacci, Chem. Phys. **40**, 237 (1979).
5. For a general discussion of copper(II) stereochemistry with particular emphasis on Jahn–Teller effects, see B. J. Hathaway, Struct. Bond. **57**, 55 (1984).
6. J. Gazo, I. B. Bersuker, J. Garaj, M. Kabesová, J. Kohout, H. Langfeldarová, M. Melnik, M. Serátor and F. Valach, Coord. Chem. Rev. **19**, 253 (1976).
7. D. R. Bloomquist and R. D. Willett, Coord. Chem. Rev. **47**, 125 (1982); S. Choi and J. A. Larabee, J. Chem. Ed. **66**, 774 (1989).
8. D. Smith, Inorg. Chim. Acta **22**, 107 (1977).
9. G. Steffen, U. Kaschuba, M. A. Hitchman and D. Reinen, Z. Naturforsch. **47b**, 465 (1992).
10. B. V. Harrowfield, Solid State Commun. **19**, 983 (1976); D. Reinen, Solid State Commun. **21**, 137 (1977).
11. M. J. Riley, M. A. Hitchman and D. Reinen, Chem. Phys. **102**, 11 (1986).
12. S. Guha and L. L. Chase, Phys. Rev. B **12**, 1658 (1975).
13. D. Reinen and C. Friebel, Struct Bond. **37**, 1 (1979).
14. A. Ceulemans, D. Beyens and L. G. Vanquickenborne, J. Am. Chem. Soc. **106**, 5824 (1984).
15. R. G. McDonald, M. J. Riley and M. A. Hitchman, Inorg. Chem. **27**, 894 (1988).
16. L. J. Basile, J. R. Ferraro, P. La Bonville and M. C. Wall, Coord. Chem. Rev. **11**, 21 (1973).
17. J. A. McGinnety, J. Am. Chem. Soc. **94**, 8406 (1972); N. Bonamies, G. Dessy and Vaciago, Theor. Chim. Acta **7**, 367 (1967).
18. R. L. Harlow, W. J. Wells III, G. W. Watt and S. H. Simonsen, Inorg. Chem. **13**, 2106 (1974).
19. R. E. Dietz, H. Kamimura, M. D. Sturge and A. Yariv, Phys. Rev. **132**, 1559 (1963).
20. S. R. Desjardins, K. W. Penfield, S. L. Cohen, R. L. Musselman and E. I. Solomon, J. Am. Chem. Soc. **105**, 4590 (1983).

21. L. Morpugo, L. Calabresi, A. Desideri and G. Rotilio, Biochem. J. **193**, 639 (1981).
22. M. Bacci, Chem. Phys. **88**, 39 (1984).
23. C. D. Flint, Coord. Chem. Rev. **14**, 47 (1974); M. Ciéslak-Golonka and A. Bartecki, Coord. Chem. Rev. **31**, 251 (1980).
24. M. A. Hitchman, Transition Met. Chem. (N.Y.) **9**, 1 (1985).
25. L. L. Lohr, J. Chem. Phys. **50**, 4596 (1969).
26. R. L. Belford and J. W. Carmichael, J. Chem. Phys. **46**, 4515 (1967); M. A. Hitchman and R. L. Belford, Inorg. Chem. **10**, 984 (1971).
27. M. A. Hitchman and P. Cassidy, Inorg. Chem. **18**, 1745 (1979).
28. R. G. McDonald and M. A. Hitchman, Inorg. Chem. **25**, 3273 (1986).
29. M. J. Riley and M. A. Hitchman, Inorg. Chem. **26**, 3205 (1987).
30. R. G. McDonald, M. J. Riley and M. A. Hitchman, Chem. Phys. Letters **142**, 529 (1987).
31. R. G. McDonald, M. J. Riley and M. A. Hitchman, Inorg. Chem. **28**, 752 (1989).
32. J. Ferguson, Progr. Inorg. Chem. **12**, 159 (1970).
33. M. A. Hitchman, Inorg. Chem. **21**, 821 (1982).
34. H. G. Drickamer, J. Chem. Phys. **47**, 1880 (1967); D. W. Smith, J. Chem. Phys. **50**, 2784 (1969); M. Berjemo and L. Pueyo, J. Chem. Phys. **78**, 854 (1983).
35. R. G. McDonald and M. A. Hitchman, Inorg. Chem. **29**, 3081 (1990).
36. R. G. McDonald and M. A. Hitchman, Inorg. Chem. **29**, 3074 (1990).
37. R. J. Deeth and M. A. Hitchman, Inorg. Chem. **25**, 1225 (1986).
38. M. J. Riley, M. A. Hitchman and A. wan Mohammed, J. Chem. Phys. **87**, 3766 (1987).
39. M. C. M. O'Brien, Proc. Roy. Soc. A **281**, 323 (1964).
40. D. Reinen and M. Atanasov, Magn. Resonance Rev. **15**, 167 (1991).
41. A. Ceuleman, J. Chem. Phys. **87**, 5374 (1987).
42. M. J. Riley, L. Dubicki, G. Moran and E. R. Krausz, Chem. Phys. **145**, 363 (1990); M. J. Riley, L. Dubicki, G. Moran, E. R. Krausz and I. Yamada, Inorg. Chem. **29**, 1614 (1990); K. Finnie, L. Dubicki, E. R. Krausz and M. J. Riley, Inorg. Chem. **29**, 3908 (1990); D. Reinen, G. Steffen, M. A. Hitchman, H. Stratemeier, L. Dubicki, E. R. Krausz, M. J. Riley, H. E. Mathies, K. Recker and F. Wallraufen, Chem. Phys. **155**, 117 (1991).
43. L. Dubicki, E. R. Krausz, M. J. Riley and Y. Yamada, Chem. Phys. Letters **157**, 315 (1989).
44. F. S. Ham, Phys. Rev. A **138**, 1727 (1965); **166**, 307 (1968); F. S. Ham, *Electron Paramagnetic Resonance*, ed. S. Geschwind (Plenum, New York, 1972), pp. 110–113.
45. B. Bleaney and D. J. E. Ingram, Proc. Phys. Soc. Ser A **63**, 408 (1950).
46. For a general discussion of the study of Jahn–Teller interactions by EPR spectroscopy, see H. Bill, *The Dynamical Jahn–Teller Effect in Localized Systems*, eds. Yu. E. Perlin and W. Wagner (North-Holland, Amsterdam, 1984), pp. 709–818.
47. R. E. Coffman, J. Chem. Phys. **48**, 669 (1968).
48. L. A. Boatner, R. W. Reynolds, Y. Chen and M. M. Abragam, Phys. Rev. B **16**, 86 (1977).
49. W. Low and J. T. Suss, Phys. Lett. **7**, 310 (1963).
50. I. M. Proctor, B. J. Hathaway and P. Nicholls, J. Chem. Soc. (A) 1678 (1968).
51. T. Ramasurba Reddy and R. Srinivasan, Phys. Lett. **22**, 143 (1966).

52. A. M. Zaitdinov, M. M. Zaripov, Yu. V. Yablokov and R. L. Davidovitch, Phys. Stat. Solidi (b) **78**, K69 (1976).
53. W. R. Clayton and E. A. Meyers, Cryst. Struct. Commun. **5**, 61 (1976); **5**, 63 (1976).
54. C. Friebel, V. Propach and D. Reinen, Z. Naturforsch. **31b**, 1574 (1976).
55. D. Reinen and S. Krause, Inorg. Chem. **20**, 2750 (1980).
56. M. J. Riley, M. A. Hitchman, D. Reinen and G. Steffen, Inorg. Chem. **27**, 1924 (1988) and references therein.
57. G. Steffen, D. Reinen, H. Stratemeier, M. J. Riley, M. A. Hitchman, H. E. Mathies, K. Recker, F. Wallrafen and J. R. Niklas, Inorg. Chem, **29**, 2123 (1990).
58. E. Herdtweck and D. Babel, Z. Krist. **159**, 189 (1980).
59. H. G. von Schnering, Z. Anorg. Allg. Chem. **353**, 13 (1967).
60. B. L. Silver and D. Getz, J. Chem. Phys. **61**, 638 (1974).
61. J. Whitnall, C. H. I. Kennard, J. Nimmo and F. H. Moore, Cryst. Struct. Commun. **4**, 717 (1975).
62. V. E. Petrashen, Yu. V. Yablokov and R. L. Davidovitch, Phys. Stat. Solidi (b) **101**, 117 (1980); N. W. Alcock, M. Duggan, A. Murray, A. Tyagi, B. J. Hathaway and A. Hewat, J. Chem. Soc. Dalton Trans. 7 (1984) and references therein.
63. J. H. Ammeter, H. B. Bürgi, E. Gamp, V. Sandrin-Meyer and W. P. Jensen, Inorg. Chem. **18**, 733 (1979); J. S. Wood, C. P. Keijzers, E. de Boer and A. Buttafava, Inorg. Chem. **19**, 2213 (1980).
64. C. J. Simmons, B. J. Hathaway, K. Amornjarusiri, B. D. Santasiero and A. Clearfield, J. Am. Chem. Soc. **109**, 1947 (1987).
65. C. J. Simmons, New Journal of Chemistry **17**, 77 (1993) and references therein.
66. M. Stebler and H. B. Bürgi, J. Am. Chem. Soc. **109**, 1395 (1987).
67. M. V. Sorokin and G. K. Chirkin, Sov. Phys. Sol. State **21**, 1720 (1979).
68. D. W. Smith, J. Chem. Soc. A 1498 (1970); J. K. Burdett, Inorg. Chem. **20**, 1959 (1981).
69. D. Tucker, P. S. White, K. L. Trojan, M. L. Kirk and W. E. Hatfield, Inorg. Chem. **30**, 823 (1991).
70. W. E. Hatfield, M. A. Hitchman, E. R. Krausz, R. Lindner, D. Reinen, J. Pebler, H.-H. Schmidtke, H. Stratemeier, L. ter Haar and B. Wagner, to be published.
71. H. C. Freeman, P. Ellis, W. E. Hatfield, M. A. Hitchman, D. Reinen and B. Wagner, to be published.
72. H. Stratemeier, M. A. Hitchman, M. J. Riley, J. Bebendorf, D. Reinen, E. Gamp and H. B. Bürgi, to be published.
73. N. W. Alcock, M. Duggan, A. Murray, S. Tyagi, B. J. Hathaway and A. Hewat, J. Chem. Soc. Dalton Trans. 7 (1984).
74. B. J. Hathaway and A. W. Hewat, J. Solid State Chem. **51**, 364 (1984).
75. C. J. Simmons, M. A. Hitchman, H. Stratemeier and A. J. Schultz, J. Am. Chem. Soc., in press.